SURGERY IN MEMBRANE FUSION

ALEJANDRO JOSÉ SOTO FRANCO

Abstract. The Gaussian curvature term of the Helfrich energy is topological, so a theory posed at fixed topological type discards it. Membrane fusion is a sequence of topology changes, and we determine what that term carries along one. The two leaflets divide a pathway's surfaces into two classes, and the class imbalance Δ, the difference of their director degrees, is insensitive to lipid tilt of any magnitude, equals the difference of the two classes' surgery numbers, and has the parity of their sum, so hemifusion is an odd surgery number. A pore rim has $\int K\,\mathrm{d}A = -4\pi$ whatever its profile and its radii. Under a single saddle-splay modulus the energy depends on the surgery number alone, and one surgery is 91 to 119 k_BT at the measured modulus; that quantity enters no line tension, and the rim whose energy it is exists only after the nucleation barrier is crossed, so neither quantity reported for a pore bears on it. A bilayer of half-thickness ℓ has $\sup|K| < \ell^{-2}$ and bending energy nonincreasing along the constrained gradient flow, every topology change requires $\mathcal{W} \geq 8\pi$, and a merge dissipates at least $4\pi - \int_N (H^2 - K)\,\mathrm{d}A$, so the whole pathway performs at most $\mathcal{W}(0)/2\pi - \chi(0)/2 - 1$ events, which k round vesicles attain.

1. Introduction

Two lipid membranes that fuse pass through a sequence of intermediates. Each membrane is a bilayer of two monolayers, or leaflets, and when two vesicles are brought into apposition the leaflets facing the gap between them are called *proximal* and the leaflets facing away *distal.* Fusion begins when the two proximal leaflets merge along a narrow neck, the stalk; the stalk expands radially, bringing the two distal leaflets into contact across a single new bilayer, the hemifusion diaphragm; and fusion completes when a pore opens inside that diaphragm, joining the two distal leaflets and the two interior compartments. The diaphragm is an intermediate: it forms, and it then decays by nucleating that pore within itself [KCK02].

Chernomordik and Kozlov review the process and the elastic models built for it [CK08], and the stalk and the diaphragm are treated quantitatively by Kozlovsky and Kozlov [KK02] and by Kozlovsky, Chernomordik and Kozlov [KCK02].

Date: 23 August 2026.

2020 *Mathematics Subject Classification.* Primary 53A05; Secondary 49Q10, 53Z05, 92C05.

Key words and phrases. Gaussian curvature, Gauss–Bonnet, Willmore energy, Willmore flow, membrane fusion, saddle-splay modulus, surgery, cobordism.

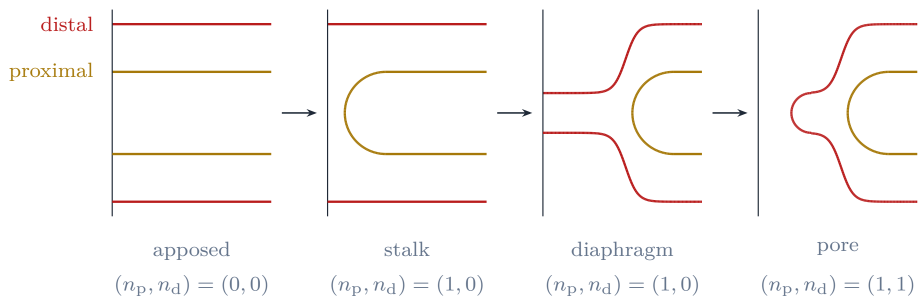

FIGURE 1. The fusion pathway in meridional half-section, each panel to be turned about the axis on its left. Proximal monolayers are drawn in gold and distal in red, and the two classes overlap in radius throughout, being separated in height. Every turn is a half-circle meeting its two faces tangentially, so its tube radius equals their half-separation. The stalk and the diaphragm have the same pair $(1, 0)$: a diaphragm is a stalk whose neck has widened, and no second surgery has occurred between them. The diaphragm is an intermediate, and it decays by nucleating the pore inside itself, which is the last transition drawn.

Two features of this sequence matter here. Every step changes the topology of the surfaces involved, and the steps are distinguished by *which* leaflets merge. A stalk merges two proximal leaflets and a pore merges two distal ones, while the failure mode in which a vesicle ruptures merges a proximal leaflet with a distal one. The Euler characteristic of the whole configuration does not separate these, and the leaflet partition does.

The standard continuum model assigns to a closed membrane surface Σ the Helfrich energy [Hel73]

$$E[\Sigma] \;=\; 2\kappa \int_\Sigma (H - c_0)^2 \,\mathrm{d}A \;+\; \bar{\kappa} \int_\Sigma K \,\mathrm{d}A, \tag{1}$$

with H the mean curvature, K the Gaussian curvature, c_0 the spontaneous curvature, κ the bending modulus and $\bar{\kappa}$ the saddle-splay, or Gaussian, modulus. At $c_0 = 0$ the first term is the Willmore energy up to normalisation, and the variational theory of Eq. (1) is well developed at fixed topology. Willmore minimisers exist within each fixed genus, by Simon for the torus and by Bauer and Kuwert above it, and the minimum over all surfaces of genus one is attained by the Clifford torus, which is the Willmore conjecture proved by Marques and Neves [MN14]. Under the constraint fixing the isoperimetric ratio, which is what a vesicle of given area and enclosed volume imposes, Schygulla proved existence of a minimiser of sphere type at every ratio [Sch12]; Keller, Mondino and Rivière extended that to every genus below 8π [KMR14], and Kusner and McGrath built the comparison surface that puts every genus and every ratio below 8π [KM21], so the constrained minimiser exists throughout. At fixed area and total mean curvature the same holds, by Scharrer and West [SW25]. For the evolution, Rupp, Scharrer and Schlierf give global existence and convergence for the constrained gradient flow below energy thresholds they compute [RSS24].

In each of these the second term of Eq. (1) plays no part. On a closed surface the Gauss–Bonnet theorem gives $\int_\Sigma K \, \mathrm{d}A = 2\pi\chi(\Sigma)$, so that term equals $2\pi\bar{\kappa}\,\chi(\Sigma)$ and is constant on each topological type. Fixing the type reduces Eq. (1) to its first term, and the saddle-splay modulus never enters; Rupp, Scharrer and Schlierf drop it for this reason, and it is dropped throughout the literature just cited. Membrane fusion is a sequence of topology changes, so along a fusion pathway that term varies. It is the only part of Eq. (1) that responds to the topology at all, and its behaviour across a change of type is what we describe.

We attach two integers to a fusion pathway and determine what each of them governs. The surfaces of a pathway divide into the proximal and distal classes of Section 2. A monolayer has a unit *director* field giving the mean orientation of its molecules, which agrees with the surface normal where the molecules stand normal to the surface and tilts away from it where they do not, and Δ is the difference of the two classes' director degrees. In Section 3 that degree is shown to be a homotopy invariant of the director field, so that Δ is insensitive to lipid tilt of any magnitude, and

$$\Delta \;=\; n_{\mathrm{d}} - n_{\mathrm{p}}, \qquad n_{\mathrm{p}} + n_{\mathrm{d}} \;\equiv\; \Delta \pmod 2,$$

where n_c is the number of surgeries performed on class c. Hemifusion is therefore an odd surgery number, and no intermediate shape has to be identified to detect it.

Section 4 evaluates the integral one topology change contributes, and the computation reduces to a single identity for surfaces of revolution. From it the -4π of a pore rim is seen to be independent of the rim's profile, of its two radii, and of which surface inside a leaflet of finite thickness is taken to represent it. A hemifusion diaphragm has two such rims, in the sense made precise there, and hence -8π.

Section 5 treats the region a pathway sweeps in $\mathbb{R}^3 \times [0, T]$, given the product metric. The region one leaflet class sweeps is a compact oriented cobordism between the initial and final surfaces of that class, on which the time function is a Morse function whose critical points are the surgeries. The bordism class of the endpoints distinguishes nothing, since every closed oriented surface bounds, so what Δ measures is a property of the cobordism with its handle decomposition. Halving the Euler characteristic of an odd-dimensional cobordism gives the surgery number a second time, without reference to the director degree. That region is also a hypersurface in flat four-space, and its scalar curvature reduces by the Gauss equation to twice the Gaussian curvature of the slice at any instant at which the flow stops, so the saddle-splay integrals below are the static part of a curvature integral over it. The surgery number is then a curvature integral over the boundary of the swept region. Section 6 determines which of the two integers the energy resolves: under a single modulus it is a function of their sum, so Δ retains the information the energy discards, and Δ enters the energy exactly when the two classes have different moduli. Section 6.3 evaluates the energy of one surgery at the measured modulus and compares the result with the measured barrier for pore nucleation. Section 6.4 restores the tension term the rest of that section sets to zero, which turns the open-pore energy into a barrier. That barrier is in the hundreds of $k_B T$ at every line tension anyone has measured, so the rim is reached after the barrier and not at it.

Section 7 bounds the Willmore energy a pathway dissipates, which is the first term of Eq. (1). A bilayer of half-thickness ℓ has every principal curvature below ℓ^{-1}, which bounds the Willmore gradient, its linearisation and the coefficients of that linearisation; along the constrained gradient flow the Willmore energy is nonincreasing, and every topology change needs $\mathcal{W} \geq 8\pi$, so all of them fall in an initial interval. The slab also forbids the pinch an ε-regularity estimate would govern, which makes an event a cut at a finite scale and the energy it dissipates computable: a merge dissipates at least 4π less the integral of $H^2 - K$ over the tube it inserts, which is positive for any tube below $4\pi\ell^2$ in area, and a fusion stalk is that object. A pore attains the bound, and returns the rim energy Section 6.3 computes by another route. The floor reaches 4π as the tube vanishes, and a pathway meeting it there performs at most $\mathcal{W}(0)/2\pi - \chi(0)/2 - 1$ events, which k round vesicles attain. Section 8 then treats the cases in which the construction fails.

The geometric input is classical, save for one estimate. Beyond Gauss–Bonnet we use the degree of the Gauss map and Hopf's theorem; Morse theory and the handle calculus of cobordisms, together with the halving of the Euler characteristic in odd dimensions; the Gauss equation for a hypersurface of a flat space, which gives Proposition 5.2; the Steiner formulae for parallel surfaces, which give Theorem 4.8; and, for the saddle-splay total at a configuration where no density represents it, curvature measures in the sense of normal cycles, following Pokorný and Rataj [PR13]. The estimate is the sharp Michael–Simon Sobolev inequality of Eq. (22), whose constant $2\sqrt{\pi}$ is Brendle's [Bre21, Cor. 2]. The thresholds 4π and 8π that Section 7 works against are Willmore's [Wil65] and Li and Yau's [LY82, Thm. 6]. We construct no minimiser and no flow. What we take from Eq. (1) is its second term, which Section 6.1 shows is the only one a topology change moves; the first enters in Section 6.3, where a measured line tension turns out to bear on the rim's bending energy, and again throughout Section 7. Existence for the full energy across a topology change rests on the constrained minimisers cited above, which exist at every genus and every ratio. What no such theorem supplies is a principle selecting the pathway between two types, and Section 8 says where that leaves the construction.

2. Leaflets, classes and pathways

2.1. **Monolayers as surfaces.** A lipid bilayer is two monolayers, each a densely packed sheet of amphiphiles whose hydrocarbon tails face those of the other. On the scale at which fusion happens the sheet is thin against every radius of curvature it takes, and the standard continuum description replaces it by a surface with a bending energy quadratic in curvature [Hel73]. The differential geometry of that description, and the stresses it implies, are set out by Deserno [Des15].

The constructions below rest on two features of it. The first is that the energy of a closed surface contains the term $\int \bar{\kappa} K \, \mathrm{d}A$, whose value is $2\pi\bar{\kappa}\chi$ and which therefore changes only when the topology does. The second is that the two monolayers are distinct surfaces: they slide against one another, they are separated by the hydrophobic core, and a quantity defined on one of them is not defined on the other. Much of the fusion literature works with the bilayer as a single surface and recovers the monolayer structure where it is needed. The constructions below need it throughout, so it is built into Definition 2.1.

Definition 2.1. A *configuration* is a finite disjoint union $\Sigma = \bigsqcup_i \Sigma_i$ of closed oriented embedded surfaces in $\mathbb{R}^3$, together with a map assigning to each component a *class*, written p for proximal and d for distal.

Assumption 2.2. Distinct monolayers are separated by the hydrophobic core or by water, and therefore share no point.

Assumption 2.2 is a statement about the physical structure and is assumed here. What it forbids is a process in its own right. Without it the two leaflets of a single bilayer could merge with each other, which is that bilayer fusing with itself; the result is again an unstable single sheet, and the pore nucleated inside it opens the membrane to its own exterior, joining no compartments. Section 8 computes what follows from that failure, so the two cases are distinguishable.

2.2. **Origin of the classes.** The classes come from the geometry of two apposed vesicles. The leaflets bounding the gap between them are proximal and the remaining two are distal, and the distinction is the organising one in the fusion literature: the stalk that opens first joins the two proximal monolayers alone, and the distal pair is untouched until later [KK02]. Reviews of the mechanism take that ordering as the definition of the pathway [CK03; CK08].

Two accounts of what follows the stalk have competed since the 1990s. In one the stalk expands radially into a hemifusion diaphragm, a single bilayer separating the two compartments, which is unstable and decays by nucleating a pore inside itself [KCK02]. In the other an inverted micellar intermediate forms and resolves directly [Sie93]. The same energetics ties both to the lamellar-to-inverted-hexagonal transition of phosphatidylethanolamine [SE97]. What separates the routes is which class acts at which step, and that is what Definition 2.1 tracks.

The Gaussian modulus that weights a topology change has been measured by simulation of a closed membrane [HBD12], by analysis of the lamellar-to-cubic transition [SK04], and by a method that reads it off a controlled change of topology [GD26]. That last is the closest prior art to what follows, since it determines the energy of a topology change from the Euler characteristic alone, with no shape entering. This paper resolves that characteristic into the two classes, and the pair of integers which results separates cases their sum does not.

2.3. **Surgeries and pathways.**

Definition 2.3. A *surgery* on a configuration replaces two components of the same class, or one component with itself, by their connected sum along an embedded handle, leaving the other components unchanged.

A surgery lowers the Euler characteristic of the affected class by 2 and preserves the partition, the resulting component inheriting the class its parents share. A merge of components of different classes admits no consistent class assignment and falls outside Definition 2.3; that case is rupture and is treated in Section 8.

Definition 2.4. A *pathway* is a family of configurations $\Sigma(t)$, indexed by $t \in [0, T]$, smooth in t away from finitely many times $0 < t_1 < \cdots < t_N < T$, at each of which one surgery occurs. Write n_{p} and n_{d} for the number of surgeries performed on each class. The *surgery number* of the pathway is $n = n_{\mathrm{p}} + n_{\mathrm{d}}$.

The pathway tracked throughout begins with two apposed vesicles, so that each class consists of two spheres. Stalk formation is one surgery on the proximal class and pore formation is one on the distal class, so complete fusion has $n_{\mathrm{p}} = n_{\mathrm{d}} = 1$ and surgery number 2, while hemifusion is the state between them, with $n_{\mathrm{p}} = 1$ and $n_{\mathrm{d}} = 0$. Definition 2.4 requires neither that the two occur in that order nor that both occur, and Section 3 shows that the order leaves a trace.

Whether a pathway of this kind arises as a solution of some dynamics is a separate question, and one the paper does not need until Section 7. The statements of Section 3 to Section 6.3 hold for any family of configurations meeting Definition 2.4, and are therefore statements about the bookkeeping of a topology change, silent on any mechanism producing one.

3. Director degree and class imbalance

A lipid monolayer has a unit director field n giving the mean orientation of its molecules. Without tilt n coincides with the surface unit normal N; in general $n = (N + t)/|N + t|$ for a tangential tilt field t.

Proposition 3.1. *Let Σ be a closed oriented surface with unit normal N, and let t be a continuous tangential field. Then* $\deg(n) = \deg(N) = \chi(\Sigma)/2$ *for every t, with no bound on $|t|$.*

Proof. Let $n_s = (N + s\,t)/|N + s\,t|$ for $s \in [0, 1]$. Since t is tangential and N is a unit normal, $|N + s\,t|^2 = 1 + s^2|t|^2 \geq 1$, so n_s is defined and continuous on $\Sigma \times [0, 1]$ and gives a homotopy from N to n. The degree of a map to $\mathbb{S}^2$ is a homotopy invariant. The value $\chi(\Sigma)/2$ for the Gauss map follows from Gauss–Bonnet together with $\int_\Sigma K\,\mathrm{d}A = 4\pi \deg(N)$. □

An expansion of $\int K\,\mathrm{d}A$ in the tilt is valid to first order, and at a fusion intermediate the correction is large. The degree requires no expansion, which is why Definition 3.3 is exact.

Remark 3.2. The homotopy requires $n \cdot N > 0$, and $n \cdot N = (1 + |t|^2)^{-1/2}$ is positive for every finite tilt. An inverted director is therefore beyond the reach of tilt of any magnitude, and this is where the degree and χ separate.

Definition 3.3. For a configuration classified as in Definition 2.1, let $D(c) = \sum_{\Sigma_i \in c} \deg(n_i)$. The *class imbalance* is $\Delta = D(\mathrm{p}) - D(\mathrm{d}) \in \mathbb{Z}$.

Theorem 3.4. *Let a pathway start from two apposed vesicles. Then at every time*

$$\Delta \;=\; n_{\mathrm{d}} \;-\; n_{\mathrm{p}}, \tag{2}$$

where n_c is the number of surgeries performed on class c up to that time.

Proof. Each class initially consists of two spheres, so $D(\mathrm{p}) = D(\mathrm{d}) = 2$ and $\Delta = 0$. By Proposition 3.1, $D(c) = \chi(c)/2$ at all times. A surgery on class c lowers $\chi(c)$ by 2, hence $D(c)$ by 1, and leaves the other class untouched. Therefore $D(\mathrm{p}) = 2 - n_{\mathrm{p}}$ and $D(\mathrm{d}) = 2 - n_{\mathrm{d}}$, and subtracting gives Eq. (2). □

Corollary 3.5. *With $n = n_{\mathrm{p}} + n_{\mathrm{d}}$, we have $n \equiv \Delta \pmod 2$. A pathway has performed an odd number of surgeries if and only if Δ is odd.*

Proof. $n - \Delta = (n_{\mathrm{p}} + n_{\mathrm{d}}) - (n_{\mathrm{d}} - n_{\mathrm{p}}) = 2n_{\mathrm{p}}$. □

For the standard pathway the values are as follows.

Table 1. Per-class surgery numbers, director degrees and class imbalance along the standard pathway.

state	n_{p}	n_{d}	$D(\mathrm{p})$	$D(\mathrm{d})$	Δ
unfused	0	0	2	2	0
stalk	1	0	1	2	−1
fused	1	1	1	1	0

Δ vanishes at both endpoints and is non-zero at hemifusion, the endpoints are separated by the total degree $4 - n$, and the sign of Δ names the route.

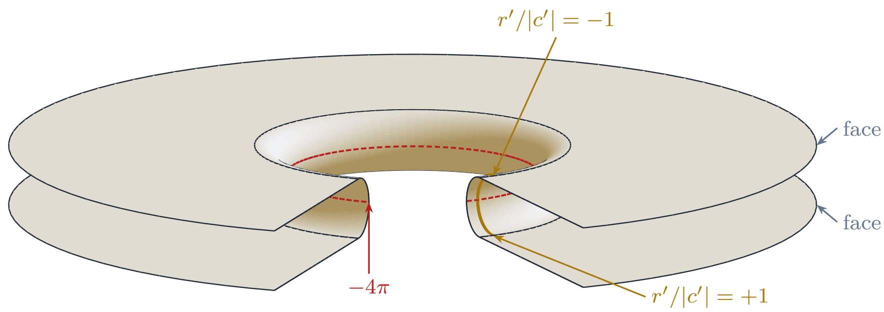

FIGURE 2. A rim as the inner half of a torus, meeting two coaxial faces radially. The profile's radial direction cosine is -1 where the tube leaves the upper face and $+1$ where it reaches the lower one, so by Lemma 4.1 the rim has $\int K\,\mathrm{d}A = -2\pi(1-(-1)) = -4\pi$ whatever the profile does between the joins. The waist, in red, is the least radius, which places the faces outside the turn and fixes the sign.

A simultaneous merge of both classes keeps $\Delta = 0$ throughout, so the imbalance detects the order of the two surgeries. Corollary 3.5 sharpens this: hemifusion is an odd surgery number, and no intermediate shape has to be inspected to detect it. The converse fails: $(3,0)$ and $(1,0)$ are both odd and differ in Δ, so parity alone leaves it undetermined.

Remark 3.6. Reversing the director convention globally flips the sign of Δ, the antipodal map having degree -1 on $\mathbb{S}^2$. That Δ vanishes at the endpoints and not at hemifusion is independent of the convention.

4. Rims

The surgeries of Section 3 are realised by rims: a monolayer arrives along one face, reverses, and departs along the other (Fig. 2). We compute the integral over a rim in Lemma 4.1 and draw four consequences from it.

Lemma 4.1. *Let Σ be the surface of revolution generated by a regular profile $s \mapsto (r(s), z(s))$ with $r > 0$, over $s \in [s_0, s_1]$. Then*

$$\int_\Sigma K\,\mathrm{d}A \;=\; -2\pi\left[\frac{r'}{\sqrt{r'^2 + z'^2}}\right]_{s_0}^{s_1}. \tag{3}$$

Proof. For such a surface

$$K = \frac{z'\,(r'z'' - z'r'')}{r\,(r'^2 + z'^2)^2}, \qquad \mathrm{d}A = r\sqrt{r'^2 + z'^2}\;\mathrm{d}s\,\mathrm{d}u,$$

so integrating over $u \in [0, 2\pi]$ gives

$$\int_\Sigma K\,\mathrm{d}A = 2\pi\int_{s_0}^{s_1}\frac{z'(r'z'' - z'r'')}{(r'^2 + z'^2)^{3/2}}\,\mathrm{d}s.$$

Differentiating $r'(r'^2 + z'^2)^{-1/2}$ and collecting terms identifies the integrand as minus that derivative, which gives Eq. (3). □

The bracketed quantity is the cosine of the angle between the profile's tangent and the radial direction, so Eq. (3) reads the integrated Gaussian curvature of a surface of revolution off the two endpoints alone.

Theorem 4.2. *Let a rim join two coaxial planar annuli tangentially, arriving radially at one and departing radially at the other. Then* $\int_{\mathrm{rim}} K\,\mathrm{d}A = -4\pi$*, independently of the profile between the joins, of the ring radius, and of the tube radius.*

Proof. Tangential arrival at the upper face gives $z' = 0$ and $r' < 0$ there, so the direction cosine is -1; departure at the lower face gives $+1$. By Lemma 4.1 the integral is $-2\pi(1 - (-1)) = -4\pi$, and neither radius enters. □

A circular arc, an elliptical arc of arbitrary aspect ratio and a polynomial profile sharing only the end slopes all give the same value, as Theorem 4.2 requires. One consequence removes a mechanism.

Corollary 4.3. *No deformation of a rim that preserves its joins changes its saddle-splay energy. A rim relaxing out of a semi-toroidal shape has the same energy as the semi-torus.*

Relaxing the tangency instead moves the curvature onto the joins, where a measure represents it.

Definition 4.4. For a piecewise-smooth closed surface Σ with smooth pieces meeting along joins, the *curvature measure* is

$$\mu \;=\; K\,\mathrm{d}A \;+\; [k_g]\,\mathrm{d}s, \tag{4}$$

the second term supported on the joins and equal to the jump in geodesic curvature across each, in the sense of normal cycles [PR13]. Gauss–Bonnet reads $\mu(\Sigma) = 2\pi\chi(\Sigma)$.

Every statement below that writes $\int K\,\mathrm{d}A$ over a configuration with joins means μ, and the two agree wherever the surface is $C^{1,1}$. The next theorem is the Lebesgue decomposition of μ on a rim.

Theorem 4.5. *Let a rim meet its faces at profile angle* $\psi \in (0, \pi/2]$*, so that the direction cosine at the ends is* $\mp \sin\psi$*. Then, for any profile, the absolutely continuous part of* μ *has mass* $-4\pi \sin\psi$*, its singular part is supported on the two junction circles and has mass* $-4\pi(1 - \sin\psi)$*, and* $\mu(\Sigma) = -4\pi$ *for every* ψ*.*

Proof. Immediate from Eq. (3), the total being pinned at -4π by Gauss–Bonnet for the closed configuration. □

Corollary 4.6. *As $\psi \to 0$ the absolutely continuous part of μ vanishes and μ converges weak-$*$ to $-4\pi\,\delta_C$, where C is the circle into which the two junctions merge. For φ continuous,*

$$\int \varphi \,\mathrm{d}\mu_\psi \;=\; -4\pi\,\varphi(C) \;+\; O(\psi),$$

the error measuring φ's variation across the rim and vanishing identically for φ constant near it. Absolute continuity fails in the limit and the mass does not.

Proof. The absolutely continuous mass is $-4\pi\sin\psi$ by Theorem 4.5, so it leaves at rate ψ, and the singular part sits at the single radius $\rho(\pi \mp \psi)$, which tends to that of C. Pairing both against φ and expanding gives the stated error. The limit sits on a circle, a set of zero area, so no density represents it: the mass per unit area on a collar about a junction diverges as the collar shrinks. □

The total is therefore independent of ψ while the decomposition is not: the whole of μ is present at breakthrough, concentrated on the junction circles, and relaxing the profile only moves it into the rim's interior. Corollary 4.6 is why the saddle-splay total is defined across a topology change, and it is used in that form in Section 6 and Section 7.

Theorem 4.7. *A hemifusion diaphragm has two rims, its pore rim and its outer rim, each an inner half-torus. Their curvatures add to -8π, independently of the diaphragm's radius and of the pore's.*

Proof. The sign of a rim's curvature is fixed by the side on which its faces lie. At a pore the membrane lies outside the turn, at radii above the waist; at the diaphragm's edge the merged proximal monolayer likewise arrives from large radius, turns, and returns. Both are inner half-tori, and Theorem 4.2 gives each -4π with no dependence on either radius. □

This is the geometric form of the statement that a rim is a handle: each changes χ by -2, so two change it by -4. The opposite half of a torus, whose faces lie inside the turn, returns $+4\pi$, and the whole torus returns zero. An independent elastic calculation reports that omitting the Gaussian term underestimates a fusion pore's energy by $-8\pi\bar{\kappa}_m$ [SK04, p. 6], the same coefficient.

A monolayer is a slab some two nanometres thick, and the integrals above are taken over a surface inside it. That choice does not matter.

Theorem 4.8. *Let Σ_t be the parallel surface at offset t. Then*

$$K_t \,\mathrm{d}A_t = K \,\mathrm{d}A, \qquad H_t \,\mathrm{d}A_t = (H - Kt)\,\mathrm{d}A, \tag{5}$$

pointwise, for every t at which Σ_t is regular.

Proof. In principal directions the shape operator of Σ_t is $S(I-tS)^{-1}$ and the area Jacobian is $\det(I-tS) = (1-tk_1)(1-tk_2)$. Hence $K_t = K/\det(I-tS)$,

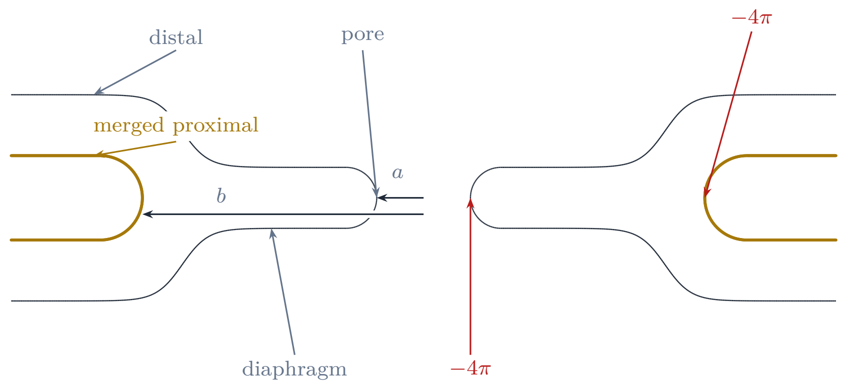

FIGURE 3. Meridional section of a hemifusion diaphragm with a pore, with the axis of revolution vertical through the centre. Outside the diaphragm's edge there are four monolayers, the two distal leaflets outermost and the merged proximal monolayer between them closing the water gap; inside the edge the two distal leaflets are in contact and form the diaphragm. Each class turns once. The distal pair turns at the pore and the proximal sheet at the diaphragm's edge, and both turns place their faces at radii above their own waist, which by Theorem 4.7 gives each of them -4π. Two radii fix the configuration: a, where the distal pair turns through the pore, and b, where the merged proximal sheet turns. Neither is written R, which Section 5 uses for a scalar curvature. The distal pair is in contact over an annulus inside b, and that annulus is the diaphragm, so a widening pore retracts it and it closes when a reaches b. The pair separates a little inside b, as the drawn flare shows, the bilayer opening over a finite width. Theorem 4.7 holds for every a and every b.

which gives the first identity, and $2H_t \det(I - tS) = k_1(1 - tk_2) + k_2(1 - tk_1) = 2H - 2tK$, which gives the second. $\square$

Corollary 4.9. *Every saddle-splay total in this paper is the same on every surface inside the leaflet. The bending term is not.*

Theorem 4.8 is classical for parallel surfaces, and Corollary 4.9 rests on the asymmetry between the two identities in Eq. (5). It also fixes the relation between the moduli of a monolayer and of its bilayer. Since $K\,\mathrm{d}A$ is invariant, two leaflets contribute exactly $2\bar{\kappa}_m K$ with no correction at any offset, and the renormalisation of the bilayer's effective saddle-splay modulus comes from the bending term. Matching coefficients of the quadratic form gives $\kappa_{bi} = 2\kappa_m$ and

$$\bar{\kappa}_{bi} \;=\; 2\bar{\kappa}_m \;+\; 8\kappa_m c_0 \delta \;+\; 4\kappa_m c_0^2 \delta^2, \tag{6}$$

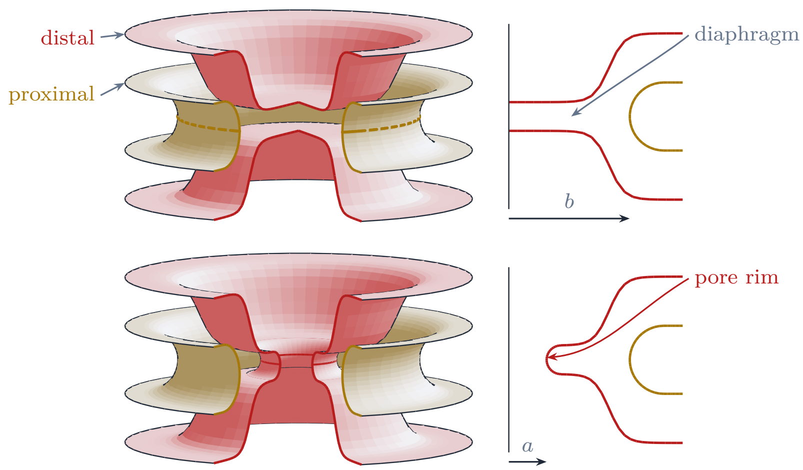

FIGURE 4. The configuration of Fig. 3 as a body of revolution with a wedge cut away, and below it the same object once a pore has nucleated in the diaphragm. Distal monolayers are red and proximal are gold, as in Fig. 1. Beside each body is its meridional half-section at the same scale, turned about the axis drawn at its left, so that the layering and the number of pieces are both legible: above, the two distal leaflets are in contact over the diaphragm and are two surfaces; below, they are one, joined round the pore's rim. That is the second surgery of Definition 2.3 seen as a change in the number of pieces, which a section alone cannot show, a section through a disc and a section through an annulus differing only in where the profile stops. The two radii a and b are the ones Fig. 3 marks, drawn here as dimension lines below each section; their values differ from that figure's because the radii are drawn at $R_{\mathrm{out}}/h_{\mathrm{out}} = 2.1$ against its 3.2, so that the pore is a fifth of the width.

whose first-order truncation is the form used in the literature [SG00, p. 2]. Reading $\bar{\kappa}_{bi}$ off the coefficient of K overcounts, since $2\kappa H^2$ contains $\kappa k_1 k_2$ of its own.

5. Geometry of the swept region

A pathway sweeps out a region of $\mathbb{R}^3 \times [0, T]$, which we give the product metric, so the ambient is flat $\mathbb{R}^4$ and nothing here is a claim about a physical spacetime; the dynamics of a membrane is a dissipative gradient flow, whose own geometry is Riemannian on a space of shapes and is not what we use.

5.1. **Cobordism and the surgery number.** Write W_c for the region the class c sweeps, that is, the union over t of $\Sigma_c(t) \times \{t\}$. Away from the

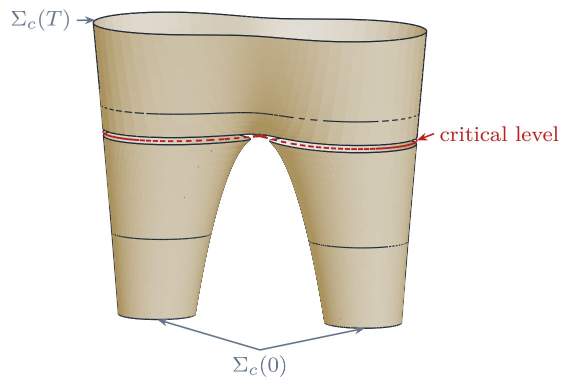

FIGURE 5. The cobordism W_c of one class, with one space dimension suppressed, so that a slice is a curve and W_c is a surface. Slices are the level sets of $((x-1)^2+y^2)((x+1)^2+y^2)$, which are two ovals below the critical value, one above it, and the lemniscate at it. The critical level is drawn in red and its node is the only critical point of the time function, of index one, since the Hessian there is $\mathrm{diag}(-4,4)$. By Proposition 5.1 the number of such points is n_c, and here it is one. Both slices at $t=0$ belong to the same class, so the merge is a surgery in the sense of Definition 2.3.

surgery times W_c is a product, and at each surgery two components of Σ_c merge along a handle. Thus W_c is a compact oriented 3-manifold with

$$\partial W_c \;=\; \Sigma_c(0) \,\sqcup\, \Sigma_c(T),$$

a cobordism between the initial and final surfaces of that class, and the time function $t\colon W_c \to [0,T]$ is a Morse function whose critical points are the surgeries. A merge of two components is an index-one critical point, and attaching a 1-handle to a 3-manifold lowers the Euler characteristic by one.

The bordism class of the endpoints distinguishes nothing. Every closed oriented surface bounds, so $\Omega_2^{SO}=0$ and any two configurations are cobordant; the same is true after the classes are remembered, since the bordism group of a two-point space is a sum of two copies of Ω_2^{SO}. What Δ measures is a property of the cobordism together with its handle decomposition, and not of the bordism class of its ends.

The Euler characteristic of an odd-dimensional compact manifold with boundary is half that of its boundary, so

$$\chi(W_c) \;=\; \tfrac{1}{2}\,\chi(\partial W_c) \;=\; \tfrac{1}{2}\big(\chi(\Sigma_c(0)) + \chi(\Sigma_c(T))\big). \tag{7}$$

Comparing this with the handle number gives a second proof of Theorem 3.4, independent of the director degree.

Proposition 5.1. *The number of surgeries performed on class c is*

$$n_c \;=\; \tfrac{1}{2}\big(\chi(\Sigma_c(0)) - \chi(\Sigma_c(T))\big),$$

and equals the number of index-one critical points of the time function on W_c.

Proof. Building W_c from the collar $\Sigma_c(0)\times[0,T]$ by attaching one 1-handle per surgery gives $\chi(W_c) = \chi(\Sigma_c(0)) - n_c$, since $\chi(\Sigma_c(0)\times[0,T]) = \chi(\Sigma_c(0))$ and each 1-handle lowers χ by one. Substituting Eq. (7) and solving for n_c gives the first claim, and the identification of n_c with the number of index-one critical points is the construction itself. □

Proposition 5.1 and Proposition 3.1 give $D(c) = \chi(\Sigma_c)/2$ at each end, so Theorem 3.4 follows again on subtracting the two classes. Equation (7) is the source of the identity: what enters the bookkeeping of a fusion pathway as a halving is the Euler characteristic of an odd-dimensional cobordism.

5.2. **Second fundamental form of the cobordism.** Let Σ_t move by a normal velocity v, so that W_c is immersed by $X(u,t) = (F(u,t),t)$ with $\partial_t F = vN$ and N the unit normal of the slice. Write $\varpi = (1+v^2)^{1/2}$, let h_{ab} be the second fundamental form of Σ_t with respect to N, and let K and H be its Gaussian and mean curvature, so $\operatorname{tr} h = 2H$ and $\det(h^a{}_b) = K$. The frame $E_a = (\partial_a F, 0)$, $E_T = (vN, 1)$ gives

$$g_W \;=\; g_\Sigma \oplus \varpi^2\,\mathrm{d}t^2, \qquad \nu \;=\; \frac{(N,-v)}{\varpi}, \qquad A \;=\; \frac{1}{\varpi}\begin{pmatrix} h_{ab} & \partial_a v \\ \partial_b v & \partial_t v \end{pmatrix}. \tag{8}$$

The metric is block diagonal, which is what makes the frame adapted, and A splits into the second fundamental form of the slice, the surface gradient of the normal speed, and the normal acceleration. Two pathways through the same instantaneous surface can share the first block and differ in the second, so a cobordism has data no slice determines.

Since the ambient is flat, the Gauss equation gives the intrinsic curvature of W from A alone, and its scalar curvature is $R_W = (\operatorname{tr} S)^2 - |S|^2 = 2\sigma_2(S)$ for $S = g_W^{-1}A$.

Proposition 5.2. *In the frame Eq.* (8)*,*

$$R_W \;=\; \frac{2K}{\varpi^2} \;+\; \frac{2\big(2H\,\partial_t v - |\nabla v|^2\big)}{\varpi^4}. \tag{9}$$

Proof. Work at a point in an orthonormal frame of the slice, so $g_\Sigma = I$ and $h = \operatorname{diag}(k_1,k_2)$. Then $S^a{}_b = h^a{}_b/\varpi$, $S^a{}_T = \nabla^a v/\varpi$, $S^T{}_b = \nabla_b v/\varpi^3$ and $S^T{}_T = \partial_t v/\varpi^3$. Now $\sigma_2(S)$ is the sum of the principal 2×2 minors. The minor on the slice directions is $\det(h/\varpi) = K/\varpi^2$, and the two minors pairing a slice direction with T sum to

$$\sum_a \big(S^a{}_a S^T{}_T - S^a{}_T S^T{}_a\big) \;=\; \frac{(\operatorname{tr} h)\,\partial_t v - |\nabla v|^2}{\varpi^4} \;=\; \frac{2H\,\partial_t v - |\nabla v|^2}{\varpi^4}.$$

Doubling the sum gives Eq. (9). □

Corollary 5.3. *At an instant at which $v = 0$ and $\nabla v = 0$,*

$$R_W \;=\; 2K + 4H\,\partial_t v.$$

The scalar curvature of W_c is twice the Gaussian curvature of the slice exactly when the normal acceleration vanishes as well.

A surface at rest is therefore not enough: a unit sphere with $v = 0$ and $\partial_t v = 1$ has $R_W = 6$ against $2K = 2$. The cobordism has to be at rest to second order, which is the same condition under which its Gauss–Kronecker density vanishes, since $\det S = (K\,\partial_t v - k_1(\nabla_2 v)^2 - k_2(\nabla_1 v)^2)/\varpi^5$ depends on the acceleration and not on the velocity.

Every saddle-splay integral in this paper is the static part of a curvature integral over W_c. Against slice area and time the density is $K/\varpi + (2H\partial_t v - |\nabla v|^2)/\varpi^3$, so for a traversal in which v, ∇v and $\partial_t v$ are all of order ε the correction to K is $2H\,\partial_t v$ at order ε, and $-|\nabla v|^2 - \frac{1}{2}Kv^2$ at order ε^2. The acceleration is felt first. The kinetic term has the opposite sign, so the correction has no fixed sign along a pathway and bounds nothing on its own.

5.3. **Curvature integral for the slab.** Let $\Omega \subset \mathbb{R}^4$ be the region the whole pathway sweeps, whose boundary consists of the two cobordisms W_{p} and W_{d}, two end caps, and the corners where these meet. Since Ω is a compact domain in flat $\mathbb{R}^4$, the interior Chern–Gauss–Bonnet integrand vanishes and Hopf's theorem gives

$$\chi(\Omega) \;=\; \deg(\nu) \;=\; \frac{1}{2\pi^2}\int_{\partial\Omega} \det(\mathrm{d}\nu)\;\mathrm{d}\sigma, \tag{10}$$

with ν the outward Gauss map and $2\pi^2$ the volume of $\mathbb{S}^3$. The integrand is the determinant of the differential of ν. On a boundary of odd dimension that differs in sign from the determinant of the shape operator, so we fix the convention by the unit sphere, where $\mathrm{d}\nu$ is the identity and Eq. (10) returns $\chi(B^4) = 1$.

Theorem 5.4. *For a pathway whose components only merge,*

$$\frac{1}{2\pi^2}\int_{W_{\mathrm{p}}\cup W_{\mathrm{d}}} \det(\mathrm{d}\nu)\;\mathrm{d}\sigma \;=\; -\tfrac{1}{2}\,n.$$

For a static pathway every smooth piece of $\partial\Omega$ has $\det(\mathrm{d}\nu) = 0$, so all of χ sits in the corners, and what they give is Eq. (7) again. This is Definition 4.4 one dimension up: the integrand over the smooth pieces is the absolutely continuous part and the singular part sits in the corners, and a static pathway is the extreme case in which the first vanishes. The pathway of Theorem 5.4 is the opposite one, where the corners contribute nothing new and the mass sits on $W_{\mathrm{p}} \cup W_{\mathrm{d}}$.

5.4. **Degree of the gradient.** Theorem 5.4 constrains the two cobordisms together. To divide it between them we compute what one transition contributes, which is a local question with a closed answer. Each W_c is locally a graph over its three-dimensional slice-and-time coordinates, so it suffices to treat

$$W \;=\; \big\{\,(x, f(x)) \,:\, x \in \mathbb{R}^3\,\big\} \;\subset\; \mathbb{R}^4. \tag{11}$$

Write $\deg(\nabla f)$ for the degree of ∇f as a proper map $\mathbb{R}^3 \to \mathbb{R}^3$, which is defined whenever $|\nabla f| \to \infty$ at infinity.

Lemma 5.5. *Let $f\colon \mathbb{R}^3 \to \mathbb{R}$ be smooth with ∇f proper. Then the graph Eq.* (11) *satisfies*

$$\frac{1}{2\pi^2}\int_W \det(\mathrm{d}\nu)\,\mathrm{d}\sigma \;=\; \tfrac{1}{2}\deg(\nabla f).$$

Proof. Let $H \subset \mathbb{S}^3$ be the open hemisphere on which the last coordinate is negative, and let $\Phi\colon \mathbb{R}^3 \to H$ send y to $(y, -1)/(1 + |y|^2)^{1/2}$, which is an orientation-preserving diffeomorphism. The unit normal of Eq. (11) with negative last component is $\nu = (\nabla f, -1)/(1+|\nabla f|^2)^{1/2}$, that is, $\nu = \Phi \circ \nabla f$. Now $\det(\mathrm{d}\nu)\,\mathrm{d}\sigma$ is the pullback under ν of the volume form of $\mathbb{S}^3$, so its integral counts the volume of H with multiplicity and sign, giving $\deg(\nabla f)\cdot \mathrm{vol}(H)$. A hemisphere has half the volume of the sphere, so $\mathrm{vol}(H) = \pi^2$, and dividing by $2\pi^2$ gives the statement. □

Nothing in the proof asks that the critical points of f be nondegenerate, or that they be isolated. The Morse case is the specialisation.

Corollary 5.6. *At a nondegenerate critical point of index λ the Morse lemma writes f in suitable coordinates as*

$$f \;=\; a_1x_1^2 + a_2x_2^2 + a_3x_3^2, \qquad a_i = \pm 1,$$

with λ the number of negative signs. Then $\nabla f = 2(a_1x_1, a_2x_2, a_3x_3)$ has degree $a_1a_2a_3 = (-1)^\lambda$, so the contribution is $(-1)^\lambda/2$.

Two graphs lie outside the Morse case. In $f = x_1^2 + x_2^2 - x_3^4$ the Hessian drops rank at the origin, and the level sets pass from two components to one, so this is a merge that the Morse lemma does not describe. Its gradient $(2x_1, 2x_2, -4x_3^3)$ is a homeomorphism of degree -1, and it contributes $-\frac{1}{2}$, as a nondegenerate merge does. The monkey saddle $f = x_1^3 - 3x_1x_2^2 - x_3^2$ has $\deg(\nabla f) = 2$ and contributes $+1$, with no merge anywhere in it. The value follows the degree of the gradient.

5.5. **Division of the degree between the classes.**

Proposition 5.7. *For a pathway whose components only merge, and for each class c,*

$$\frac{1}{2\pi^2}\int_{W_c} \det(\mathrm{d}\nu)\,\mathrm{d}\sigma \;=\; \tfrac{1}{2}\,\chi\big(W_c, \Sigma_c(0)\big) \;=\; -\tfrac{1}{2}\,n_c.$$

Proof. The time function on W_c is Morse, and away from its critical points it is locally a product $\Sigma \times I$. There the normal is constant along the I factor, so $\mathrm{d}\nu$ has a kernel and $\det(\mathrm{d}\nu) = 0$; the degree comes from the critical points alone. Summing Lemma 5.5 over them gives $\frac{1}{2}\sum_p (-1)^{\lambda(p)}$, which is half the relative Euler characteristic $\chi(W_c, \Sigma_c(0))$. Every critical point of a merge has index one by Proposition 5.1, so the sum is $-n_c$. □

Summing Proposition 5.7 over the two classes returns Theorem 5.4, since $n = n_{\mathrm{p}} + n_{\mathrm{d}}$. Subtracting them gives the statement this section has been assembling.

Theorem 5.8. *For a pathway whose components only merge,*

$$\frac{1}{2\pi^2}\left[\int_{W_{\mathrm{d}}} \det(\mathrm{d}\nu)\,\mathrm{d}\sigma \;-\; \int_{W_{\mathrm{p}}} \det(\mathrm{d}\nu)\,\mathrm{d}\sigma\right] \;=\; -\tfrac{1}{2}\,\Delta.$$

Proof. Apply Proposition 5.7 to each class and use $\Delta = n_{\mathrm{d}} - n_{\mathrm{p}}$ from Theorem 3.4. □

Theorem 5.8 identifies the class imbalance with the asymmetry of a curvature integral. Δ was defined in Section 3 by a degree attached to the director field on a surface; here it is the failure of two four-dimensional curvature integrals to agree.

Corollary 5.9. *The two cobordisms have equal curvature exactly when* $\Delta = 0$*, and each then has* $-\frac{1}{2}n/2$.

The fusion pathway has $n_{\mathrm{p}} = n_{\mathrm{d}} = 1$, so its two cobordisms have $-\frac{1}{2}$ apiece and the division reads as a symmetry of the pathway. That is a coincidence of its two surgery numbers. Hemifusion has $n_{\mathrm{p}} = 1$ and $n_{\mathrm{d}} = 0$, so one has $-\frac{1}{2}$ and the other has nothing, and the division is as uneven as it can be. By Corollary 3.5 the parity of the sum detects hemifusion; by Theorem 5.8 the difference detects which class has acted.

6. Membrane energy along a pathway

A pathway is described by the pair $(n_{\mathrm{p}}, n_{\mathrm{d}})$ of per-class surgery numbers, or equivalently by the surgery number $n = n_{\mathrm{p}} + n_{\mathrm{d}}$ and the class imbalance $\Delta = n_{\mathrm{d}} - n_{\mathrm{p}}$ of Theorem 3.4. The change of basis is unimodular, so the two descriptions contain the same information. This section places the saddle-splay term inside the functional it belongs to, computes the energy as a function of that pair, determines which of the two coordinates the energy resolves, and sets the result against the measured energetics of pore formation.

6.1. Canham–Helfrich energy.

Equation (1) is what remains of the membrane energy at fixed area and fixed enclosed volume. In full, with a tension σ and a pressure difference Δp, the functional is

$$\mathcal{F}[\Sigma] \;=\; 2\kappa\int_{\Sigma}(H - c_0)^2\,\mathrm{d}A \;+\; \bar{\kappa}\int_{\Sigma} K\,\mathrm{d}A \;+\; \sigma\,|\Sigma| \;+\; \Delta p\, V, \qquad (12)$$

the Canham–Helfrich energy [Hel73; RSS24]. Expanding the square and applying Gauss–Bonnet to the second term,

$$\mathcal{F} \;=\; 2\kappa\,\mathcal{W} \;-\; 4\kappa c_0 \int_\Sigma H\,\mathrm{d}A \;+\; \big(2\kappa c_0^2 + \sigma\big)|\Sigma| \;+\; 2\pi\bar\kappa\,\chi(\Sigma) \;+\; \Delta p\,V. \quad (13)$$

Every term of Eq. (13) is an object already in this paper. The first is the Willmore energy of Section 7. The second is the area difference of Corollary 7.16: since $A_+ - A_- = -4\ell \int H\,\mathrm{d}A$, the spontaneous-curvature term equals $(\kappa c_0/\ell)(A_+ - A_-)$, so area-difference elasticity [Mia+94] is Eq. (12) read in different letters. The last three are weighted by the quantities Proposition 7.17 fixes. The constrained flow of Definition 7.1 is therefore the gradient flow of Eq. (12) at fixed volume, area and area difference, which is the vesicle-shape problem as it is posed in the literature [RSS24].

Proposition 6.1. *Along a pathway the only term of Eq.* (13) *discontinuous at a surgery is* $2\pi\bar\kappa\chi$. *Its jump is* $-4\pi\bar\kappa$, *and it is independent of* κ, c_0, σ *and* Δp.

Proof. $\mathcal{W}$, $\int H\,\mathrm{d}A$, $|\Sigma|$ and V are integrals of densities bounded by Lemma 7.6 over a domain whose measure varies continuously, and Corollary 4.6 extends each across the singular instant. An index-one surgery lowers χ by 2 by Definition 2.3. □

Proposition 6.1 is what makes a saddle-splay accounting possible at all. Whatever the other four moduli are, and however the surface is shaped, the discontinuity of the membrane energy along a pathway is $4\pi|\bar\kappa|$ per surgery.

6.2. **Energy of a pathway.**

Theorem 6.2. *Let each surgery on class* c *be weighted by a modulus* $\bar\kappa_c$, *so that its saddle-splay energy is* $4\pi|\bar\kappa_c|$, *and write* $k_c = |\bar\kappa_c|$. *Then*

$$E \;=\; 4\pi\,(k_\mathrm{p} n_\mathrm{p} + k_\mathrm{d} n_\mathrm{d}) \;=\; 2\pi\big[(k_\mathrm{p} + k_\mathrm{d})\,n \;+\; (k_\mathrm{d} - k_\mathrm{p})\,\Delta\big]. \qquad (14)$$

If $k_\mathrm{p} = k_\mathrm{d} = k$ *then* $E = 4\pi k n$, *a function of the sum alone, and* $\partial E/\partial\Delta = 0$.

Proof. Substitute $n_\mathrm{p} = (n-\Delta)/2$ and $n_\mathrm{d} = (n+\Delta)/2$, which is Theorem 3.4. □

Corollary 6.3. *Under a single modulus, two pathways with the same surgery number and different class imbalances have the same saddle-splay energy, and two pathways with the same imbalance and different surgery numbers do not. The energy and the class imbalance are independent coordinates on* $(n_\mathrm{p}, n_\mathrm{d})$.

By Corollary 6.3 the class imbalance retains the information the saddle-splay term discards. By Eq. (14) it enters the energy exactly when the two classes differ in modulus, with coefficient $2\pi(\bar\kappa_\mathrm{d} - \bar\kappa_\mathrm{p})$. The same difference of moduli weights the transfer in Theorem 4.5, where a common value cancels.

One constant would therefore both give the energy of a rim's relaxation and allow Δ to be read from a measured energy.

Equation (14) is a statement about a pathway that passes through configurations at which the saddle-splay integrand is not a function, so it needs Definition 4.4 to be well posed. What Theorem 6.2 evaluates is $\mu(\Sigma_c)$, whose value is $2\pi\chi(\Sigma_c)$ at every instant including the singular ones, and Corollary 4.6 is what extends it across them: the mass is what the class imbalance is read from and the density is what the limit loses. An energy that read the integrand pointwise would have nothing to evaluate at a surgery.

6.3. **Rim energy against the measurement.** Theorem 6.2 converts the surgery number into an energy through one constant. This subsection states the constant, computes the rest of the rim's energy, and identifies which of the two the measurements test.

The monolayer saddle-splay modulus has been measured twice for lipids of the fusion-relevant class. Simulation of a closed membrane gives $\bar{\kappa}_m/\kappa_m = -0.93 \pm 0.05$ [HBD12, p. 5], and analysis of the lamellar-to-cubic transition of DOPE-Me gives -0.83 ± 0.08 [SK04, p. 4, Eq. 12]. The separation is 0.10 against a combined uncertainty of 0.094, so the two agree to 1.06 standard deviations. Both lie inside the admissible range $(-1, 0)$ [She+06]. Two is the number available: the width of the interval below is the uncertainty on those two measurements, and the methods proposed since report no value for these lipids, one measuring the modulus off a controlled change of topology [GD26] and one off the stress–strain relation of a buckling disc [Wan+24]. With $\kappa_m = 9.66\,k_BT$, Theorem 4.2 puts one surgery at $4\pi|\bar{\kappa}_m|$, which is 91 to $119\,k_BT$ across the two intervals.

Those are monolayer quantities, and the fusion literature reports a bilayer one. The two accountings coincide. A bilayer fusion performs two surgeries, one on each class, so Theorem 6.2 weighs it by $8\pi|\bar{\kappa}_m|$ under a single modulus, and Eq. (6) at $c_0 = 0$ gives $\bar{\kappa}_{bi} = 2\bar{\kappa}_m$, so the bilayer jump $-4\pi\bar{\kappa}_{bi}$ is the same number and not a second estimate of it. Numerically it is 182 to $238\,k_BT$, against the $250\,k_BT$ quoted from a bilayer modulus rounded to $-20\,k_BT$ [Bot+24, p. 2]; Eq. (6) puts κ_{bi} at $19.3\,k_BT$ here, and that rounding accounts for the difference. The two accountings agree identically because $K\,\mathrm{d}A$ is the invariant of Theorem 4.8: the two leaflets contribute $2\bar{\kappa}_m K$ at any offset, which is why Eq. (6) has no correction in $\bar{\kappa}$ and every correction in κ.

By Proposition 6.1 that quantity is a constant offset in the free energy of an open pore. It is not a barrier, and the state at which a nucleation barrier is reported has no rim: the free energy landscapes computed for eight biological membranes define ΔG_{nuc} at a reaction coordinate $\xi_p = 0.92$, which is the state with a thin transmembrane water wire, while the toroidal pore appears only near $\xi_p \approx 1.5$ [SAH25, pp. 3–4]. The quantity to compare against is the open-pore branch, and on that branch the saddle-splay term is one of two contributions. The other follows from the same geometry.

Proposition 6.4. *Let the rim of Theorem 4.2 have pore radius R and tube radius ℓ, and write $\rho = R/\ell > 1$. At $c_0 = \sigma = \Delta p = 0$,*

$$\mathcal{F}_{\mathrm{rim}} \;=\; \pi\kappa\big[\rho^2 I(\rho) - 8\big] \;-\; 4\pi\bar{\kappa}, \qquad I(\rho) \;=\; \frac{2}{\sqrt{\rho^2-1}}\Big[\pi - 2\arctan\sqrt{\tfrac{\rho-1}{\rho+1}}\,\Big]. \tag{15}$$

Setting $v = \pi + w$ gives $I(\rho) = \int_{-\pi/2}^{\pi/2}(\rho - \cos w)^{-1}\,\mathrm{d}w = \sum_{n\ge 0} c_n \rho^{-(n+1)}$ with $c_n = \int_{-\pi/2}^{\pi/2}\cos^n w\,\mathrm{d}w > 0$, convergent for every $\rho > 1$, so

$$\frac{\pi}{2\rho} \;\le\; \rho^2 I(\rho) - \pi\rho - 2 \;\le\; \frac{\pi}{2(\rho-1)}, \tag{16}$$

and therefore

$$\mathcal{F}_{\mathrm{rim}} \;=\; 2\pi R\cdot\frac{\pi\kappa}{2\ell} \;-\; 2\pi\big(3\kappa + 2\bar{\kappa}\big) \;+\; \pi\kappa\, r(\rho), \qquad \frac{\pi}{2\rho} \le r(\rho) \le \frac{\pi}{2(\rho-1)}. \tag{17}$$

The c_n do not sum, so $\mathcal{F}_{\mathrm{rim}} \to \infty$ as $\rho \to 1$.

Proof. On the inner half of the torus $2H = (R + 2\ell\cos v)/\big(\ell(R + \ell\cos v)\big)$ and $\mathrm{d}A = \ell(R + \ell\cos v)\,\mathrm{d}v\,\mathrm{d}\varphi$, so the bending density integrates to $(\pi\kappa/\ell)\int_{\pi/2}^{3\pi/2}(R + 2\ell\cos v)^2/(R + \ell\cos v)\,\mathrm{d}v$. The integrand divides exactly as $4\ell\cos v + R^2/(R + \ell\cos v)$, whose first part contributes -8ℓ and whose second contributes $R^2 I(\rho)/\ell$. The saddle-splay term is $-4\pi\bar{\kappa}$ by Theorem 4.2. For Eq. (16), the folded integrand expands as $\sum_n \cos^n w\,\rho^{-(n+1)}$, uniformly on $[-\pi/2, \pi/2]$ for $\rho > 1$; every c_n is positive, which bounds the tail below by its first term $c_2/\rho = \pi/2\rho$, and the c_n decrease, which bounds it above by $c_2\sum_{n\ge 2}\rho^{1-n} = \pi/2(\rho-1)$. □

Corollary 6.5. *Let $\rho^* = 1.5985\ldots$ be the minimiser of $\rho^2 I(\rho)$. At fixed R, $\mathcal{F}_{\mathrm{rim}}$ is stationary in ℓ exactly at $\ell = R/\rho^*$, and there $\mathcal{F}_{\mathrm{rim}} = 3.79\ldots\kappa - 4\pi\bar{\kappa}$, independent of R. A rim free to choose its tube radius has no line tension. At fixed ℓ the same ρ^* is the stationary pore radius $R = \rho^*\ell$.*

Proof. At fixed R the energy depends on ℓ through $\rho = R/\ell$ alone, so its stationary points in ℓ and in ρ coincide, and the stationary value is $\pi\kappa[\rho^{*2} I(\rho^*) - 8] - 4\pi\bar{\kappa}$, in which R does not appear. □

Equation (17) splits the rim energy into a part proportional to the rim length and a constant, and only the first is a line tension. That line tension is $\pi\kappa/2\ell$, which is the quantity the same source builds from one principal curvature $1/\ell$ over a cross-section of arc length $\pi\ell$ and correlates against its simulations at a coefficient of 0.97 [SAH25, Fig. 6h]; the two constructions agree where theirs is defined. At $\kappa_m = 9.66\,k_BT$ and $\ell = 1.4\,\mathrm{nm}$ it predicts 46 pN, against a measured range of 40 to 100 pN over the eight membranes.

The saddle-splay term is $-4\pi\bar{\kappa}$ at every R, so its derivative vanishes, and a line tension is a derivative. No measurement of a pore line tension bears on $\bar{\kappa}$ at any radius or for any lipid.

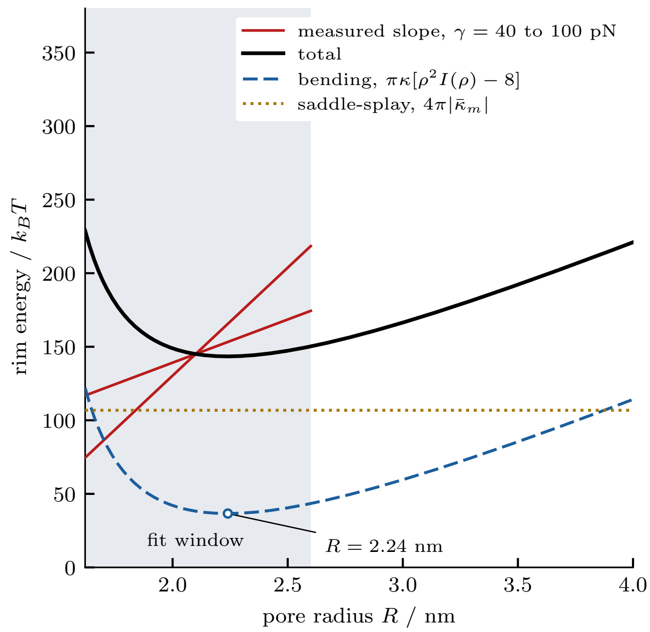

FIGURE 6. The rim energy of Eq. (15) against pore radius at $\kappa_m = 9.66\,k_BT$, $\ell = 1.4\,\mathrm{nm}$ and $\bar{\kappa}_m = -0.88\,\kappa_m$, with its two parts separated. Nothing is fitted. The saddle-splay part is level, so it shifts the curve and never its slope, and a fitted line tension measures the bending part alone. The two straight lines are the measured range of line tensions, hinged on the total at the midpoint of the window over which the measurement is fitted, so what is compared is the slope: they rise where the model falls, the bending part turning at $R = 2.24\,\mathrm{nm}$ inside that window.

Of the two quantities reported, one cannot see the saddle-splay term and the other is recorded before the rim exists. Setting $4\pi|\bar{\kappa}_m|$ against ΔG_{nuc} compares a completed surgery's topological constant with a state that has not performed one, and the two do not measure the same thing. Figure 6 draws the rim energy with its two parts separated, which is where that is visible.

What the measurement does bear on is the bending term, and there the agreement holds only where Eq. (17) is derived. The reported line tensions are fitted over $1.6 \le R \le 2.6\,\mathrm{nm}$, which at $\ell = 1.4\,\mathrm{nm}$ is $1.14 \le \rho \le 1.86$, and Eq. (15) is far from its asymptote there: the asymptotic split misses it by 86% at the lower end, it turns at $R = 2.24\,\mathrm{nm}$ inside the window, and a fit across the window returns a negative slope. A rim of fixed tube radius therefore predicts a pore that widens on its own at exactly the radii where the measurement finds one that resists widening. That failure is entirely in the bending part, $\bar{\kappa}$ contributing the same constant throughout.

Corollary 6.5 says what the turning point is. At $\ell = 1.4\,\mathrm{nm}$ it sits at $\rho^*\ell = 2.24\,\mathrm{nm}$, and it is the aspect ratio a rim would choose if its tube radius were free. Two things follow. A line tension exists at all only because ℓ is pinned at the monolayer thickness; a released rim has none. The pinned rim also has a stationary pore radius, so the model predicts a metastable open pore at $R = \rho^*\ell$, smaller for a thinner membrane. A metastable open pore is reported for exactly one of the membranes measured, the thinnest [SAH25, Fig. 3a].

Two remarks from the source point the same way. Helfrich theory "may be taken as a series expansion of the free energy up to second order around a flat reference geometry; thus, whether the theory is applicable to a highly curved pore rim is unclear" [SAH25, p. 7], and the rim's curvature radius is ℓ, the monolayer thickness itself. Its own bending prediction "overestimates the line tension by a factor of approximately two" [SAH25, p. 9]. Nothing in either remark is about $\bar{\kappa}$.

The saddle-splay term is also the term that model omits, and its authors say it should not be: the Gaussian modulus "is potentially relevant for pore formation" because "the formation of a pore changes the topology of the membrane and involves the formation of an additional boundary" [SAH25, p. 7]. Proposition 6.1 supplies it, and by Corollary 4.3 and Corollary 4.9 its value is unchanged by a reshaping of the rim and by a move to another surface inside the leaflet, where the bending term's value changes.

What remains empirical is the modulus. Whether $\bar{\kappa}$ takes a different value on the highly curved set where the curvature concentrates is a question about lipids, and it is the question Theorem 6.2 raises, which needs the two classes' moduli to differ. Testing it needs two things a slope cannot give: the R-independent offset of an open-pore branch, and a rim whose tube radius relaxes with the pore. The same tension appears in the literature: including the Gaussian term shifts published fusion pore energies by about $200\,k_BT$ [SK04, p. 6]. Tilt, which lies outside a surface model, is the mode the nucleation free energy is found to track, at a coefficient of 0.96 against the tilt modulus [SAH25, Fig. 6g], and at a trilaminar contact it contributes an amount equal to the bending contribution [MA02, p. 12].

6.4. **Tension and the pore barrier.** Proposition 6.4 holds at $c_0 = \sigma = \Delta p = 0$, which is why it gives an energy and no barrier. Tension is the control an experiment turns, and restoring it requires one area computation. Opening a pore removes a disc of radius R from each of the two leaflets the surgery joins and glues in the rim, so the area traded is

$$\Delta A \;=\; 2\pi\ell(\pi R - 2\ell) - 2\pi R^2 \;=\; 2\pi\ell^2\bigl(\pi\rho - 2 - \rho^2\bigr), \tag{18}$$

negative for a wide pore, so tension favours widening. Two discs are why the quadratic has 2π: σ here is a monolayer tension and a symmetric bilayer's is twice it, which returns the classical coefficient. Δp couples to an enclosed volume, and a pore releases that constraint rather than paying against it, so it does not enter a planar landscape.

Proposition 6.6. *With $\tau = \sigma\ell^2/\kappa$ the rim energy of Proposition 6.4 becomes*

$$\mathcal{F}_{\mathrm{rim}}(\rho) \;=\; \pi\kappa\big[\rho^2 I(\rho) - 8\big] - 4\pi\bar{\kappa} \;+\; 2\pi\kappa\,\tau\big(\pi\rho - 2 - \rho^2\big). \tag{19}$$

It diverges as $\rho \to 1$, has a minimum near the ρ^* of Corollary 6.5, a maximum at some $\rho_c > \rho^*$, and falls without bound beyond it. As $\tau \to 0$ the barrier between the two approaches $\pi^3\kappa/8\tau$, which is $\pi\gamma^2/\sigma_{\mathrm{bi}}$ at the line tension $\gamma = \pi\kappa/2\ell$ of Eq. (17)*.*

Corollary 6.7. *The saddle-splay modulus enters Eq.* (19) *as a constant in ρ. It therefore moves neither ρ^* nor ρ_c, and it cancels from the barrier $\mathcal{F}_{\mathrm{rim}}(\rho_c) - \mathcal{F}_{\mathrm{rim}}(\rho^*)$, which is a function of κ, ℓ and σ alone.*

Three quarters of a released rim's energy is the saddle-splay constant by Corollary 6.5, and none of it reaches the barrier to widening an existing pore. What $\bar{\kappa}$ does move is the height of the whole open-pore branch above the intact membrane, so it enters a barrier measured from the intact state and not one measured from a pore. That first leg runs through the water wire of [SAH25, pp. 3–4], which has no rim and which no surface model reaches.

Corollary 6.8. *The minimum and the maximum meet where $\mathcal{F}'_{\mathrm{rim}} = \mathcal{F}''_{\mathrm{rim}} = 0$, at $\rho = 1.7066$ and $\tau = 1.4769$. Beyond that tension the pore widens with no barrier at all, and the lysis tension is $\tau\kappa/\ell^2$.*

At $\kappa_m = 9.66\,k_BT$ and $\ell = 1.4\,\mathrm{nm}$, κ_m/ℓ^2 is 21.1 mN/m, so Corollary 6.8 puts the monolayer lysis tension at 31.2 and the bilayer one at 62.3 mN/m, against the few mN/m at which vesicles of these lipids rupture. Those two numbers answer different questions. A spinodal is where the barrier reaches nothing; a measured rupture tension is where rupture proceeds at a rate, with a barrier of order $25\,k_BT$ still standing, so a spinodal has to lie above it. The inequality is the expected one and it tests nothing.

What does test something is the barrier. At $\sigma_{\mathrm{bi}} = 4.2\,\mathrm{mN/m}$ it is $311\,k_BT$ and at 2.1 it is 683, so on this landscape nothing nucleates at any tension an experiment reaches. The cause is not the rim drawn here. To leading order the barrier is $\pi\gamma^2/\sigma_{\mathrm{bi}}$, a function of the line tension alone, and at $\gamma = 40\,\mathrm{pN}$, the low end of the measured range quoted in Section 6.3, it is still $235\,k_BT$ at 5 mN/m. A barrier a laboratory timescale would cross needs $\gamma = 13\,\mathrm{pN}$, below that whole range. No repair to the bending geometry reaches it, and $\bar{\kappa}$ has cancelled out of it by Corollary 6.7, so neither modulus is the quantity at fault.

What is at fault is the identification of the saddle. A gap between 300 and $25\,k_BT$ is a factor e^{275} in the rate, which is a statement that the membrane does not go this way, and no tuning closes it. Section 6.3 reaches the same conclusion from the measurement and without any of this: ΔG_{nuc} is defined at $\xi_p = 0.92$, a state with a water wire and no rim, while the toroidal pore appears only near $\xi_p \approx 1.5$ [SAH25, pp. 3–4]. The barrier is crossed before the rim exists. The rim is therefore a post-nucleation object, and the two arguments for that are independent: one counts the energy of the rim and one observes where the measurement is taken.

Corollary 6.5 lets the tube radius follow the pore, and doing the same here changes the problem. At $\sigma = 0$ the energy is a function of ρ alone, both of its terms being scale invariant, so the scale is free; the tension term is not scale invariant, and it fixes one.

Proposition 6.9. *Let $\mathcal{F}_{\mathrm{rim}}$ be stationary in R and in ℓ together. Then the traded area Eq.* (18) *vanishes, so*

$$\rho^2 - \pi\rho + 2 \;=\; 0, \qquad \rho_c \;=\; \tfrac{1}{2}\big(\pi + \sqrt{\pi^2 - 8}\big) \;=\; 2.2545\ldots,$$

the other root lying below 1*. Nothing enters ρ_c: neither modulus, neither length, the tension, nor any feature of the bending profile. The scale is $\ell_c = 0.9204\sqrt{\kappa/\sigma}$, the energy there is $6.9575\,\kappa - 4\pi\bar{\kappa}$ and no tension enters it, and the Hessian in (R, ℓ) has one negative eigenvalue.*

Proof. Write the energy as $\kappa g(R/\ell) + 2\pi\sigma(\pi\ell R - 2\ell^2 - R^2)$. Its two derivatives are $\kappa g'(\rho)/\ell + 2\pi\sigma\ell(\pi - 2\rho)$ and $-\kappa\rho g'(\rho)/\ell + 2\pi\sigma\ell(\pi\rho - 4)$, and ρ times the first added to the second removes g' and leaves $2\pi\sigma\ell(\pi\rho - 4 + \rho(\pi - 2\rho))$, which is twice Eq. (18). The scale then follows from either equation, $g'(\rho_c)$ being positive since ρ_c lies above the minimum ρ^*. The traded area vanishing is what removes σ from the value. □

The index is one within the two-parameter family of rims and the statement is about that family. A surface model has no coordinate for lipid tilt, hydration or a hydrophobic defect, and the paragraph above puts the membrane's own saddle among exactly those, so this is a critical point of the rim family and not a state the membrane occupies.

That the critical energy is independent of the tension is another reading of the same fact: the critical rim sits where a pore trades no area, so tension does no work there and can only move the scale, as $\sqrt{\kappa/\sigma}$. At $\kappa_m = 9.66\,k_BT$ and $\bar{\kappa}_m = -0.88\,\kappa_m$ the barrier is $174\,k_BT$, of which 107 is the saddle-splay term. A relaxed rim reverses Corollary 6.7: measured from the intact membrane rather than from an existing pore, $\bar{\kappa}$ supplies three fifths of the barrier, and it is the quantity a composition moves.

Which picture applies is a question about the lipid. A rim cannot relax past the molecule it is made of, so the relaxed critical rim is available only where $\ell_c \leq \ell$, which at these parameters is $\sigma_{\mathrm{bi}} \geq 35.7\,\mathrm{mN/m}$. Below that the critical tube radius exceeds the membrane's own half-thickness and the pinned picture is the physical one, which is the picture whose barrier is hundreds of k_BT. The two readings agree that a continuum rim does not nucleate a pore at any tension an experiment reaches, and they disagree about what would help: the pinned barrier does not see $\bar{\kappa}$ at all, and the relaxed one is mostly $\bar{\kappa}$.

One consequence bears on what a composition can reach. A composition that lowers the open pore's energy, through $\bar{\kappa}$ or through κ, acts on a state the membrane reaches after the barrier and not before it, so it moves the depth of the open-pore branch and leaves the nucleation rate where it was. The rate is set upstream of the rim, among the tilt, hydration and packing for which a surface model has no coordinate, and Section 8 is where that boundary is drawn.

7. Dissipation and topology change

Section 5 and Section 6 give the energy of a pathway of a given surgery number, and nothing so far bounds that number. This section bounds it from the energy alone, and along the way closes the correction term left indefinite in Proposition 5.2.

Throughout, $\Sigma(t)$ moves by a normal velocity of speed v, the second fundamental form is h with $\operatorname{tr} h = 2H$, and $\mathcal{W}(\Sigma) = \int_\Sigma H^2 \, \mathrm{d}A$. Under such a motion

$$\partial_t(\mathrm{d}A) \;=\; -2Hv \, \mathrm{d}A, \qquad \partial_t(2H) \;=\; \Delta v + |h|^2 v. \tag{20}$$

7.1. **Dissipation along the flow.**

Definition 7.1. Let $C \subset L^2(\Sigma, \mathrm{d}A)$ be the span of the densities conjugate to the constrained quantities, and let P be the orthogonal projection onto $C^\perp$. The pathway is a *constrained gradient flow* when $v = -P(\delta\mathcal{W})$, where $\delta\mathcal{W} = \Delta H + 2H(H^2 - K)$.

Proposition 7.2. *Along a constrained gradient flow,*

$$\frac{\mathrm{d}}{\mathrm{d}t}\mathcal{W} \;=\; -\big\|P(\delta\mathcal{W})\big\|_{L^2}^2 \;\le\; 0, \qquad \int_0^T \int_{\Sigma(t)} v^2 \, \mathrm{d}A \, \mathrm{d}t \;=\; \mathcal{W}(0) - \mathcal{W}(T).$$

Proof. The first variation pairs the gradient against the normal speed, so $\mathrm{d}\mathcal{W}/\,\mathrm{d}t \;=\; \langle \delta\mathcal{W}, v\rangle \;=\; -\langle \delta\mathcal{W}, P\delta\mathcal{W}\rangle$. Since $P = P^2 = P^\top$, that equals $-\|P\delta\mathcal{W}\|^2$, which is also $\|v\|^2$. Integrate in time. □

The projection is what makes Proposition 7.2 apply to a membrane. A vesicle conserves its enclosed volume and its area, and Proposition 7.17 below adds a third constraint; each removes one direction from the admissible velocities and none of them changes the sign.

7.2. **Integral of the correction term.**

Equation (9) has a term $2H\partial_t v - |\nabla v|^2$ of no fixed sign. Its time integral has one.

Proposition 7.3. *For a closed surface moving by a normal velocity on* $[0, T]$*,*

$$\int_0^T \int_{\Sigma(t)} \big(2H \, \partial_t v - |\nabla v|^2\big) \, \mathrm{d}A \, \mathrm{d}t \;=\; \Big[\int_{\Sigma(t)} 2Hv \, \mathrm{d}A\Big]_0^T \;+\; 2\int_0^T \int_{\Sigma(t)} K v^2 \, \mathrm{d}A \, \mathrm{d}t. \tag{21}$$

Proof. By Eq. (20), $\partial_t(2H\,\mathrm{d}A) = \big(\Delta v + (|h|^2 - 4H^2)v\big)\,\mathrm{d}A$. Integrating the first term of the left side by parts in time therefore contributes $-\iint v\Delta v - \iint(|h|^2 - 4H^2)v^2$ together with the boundary term. On a closed surface $\int v\Delta v\,\mathrm{d}A = -\int|\nabla v|^2\,\mathrm{d}A$, which cancels the kinetic term, and in two dimensions $4H^2 - |h|^2 = 2K$. $\square$

Corollary 7.4. *Along a pathway at rest at both ends the correction is* $2\iint Kv^2$, *negative exactly where the moving part of the surface is saddle-shaped. If v is constant over $\Sigma(t)$ at each instant it is* $4\pi\int_0^T \chi(\Sigma(t))\,v^2\,\mathrm{d}t$.

7.3. **Slab geometry and its curvature bound.** A bilayer is a slab. Its leaflets are the parallel surfaces of the mid-surface, and a parallel surface degenerates.

Definition 7.5. The *slab* of half-thickness $\ell > 0$ about Σ is the image of $\Sigma \times [-\ell, \ell]$ under $(x, s) \mapsto x + s\,\nu(x)$. It is *nondegenerate* when that map is an immersion.

Lemma 7.6. *The area element of the surface at distance s is* $\det(1 - sS)\,\mathrm{d}A = (1 - 2Hs + Ks^2)\,\mathrm{d}A$. *A nondegenerate slab therefore has*

$$|k_i| < \frac{1}{\ell} \quad \textit{on } \Sigma, \qquad \textit{hence} \qquad \sup_\Sigma |K| < \frac{1}{\ell^2}, \qquad \sup_\Sigma |h|^2 < \frac{2}{\ell^2}.$$

Proof. The area factor is $(1 - sk_1)(1 - sk_2)$, equal to 1 at $s = 0$. Immersion forbids either factor from vanishing on $[-\ell, \ell]$, so each keeps its sign there, which is $|sk_i| < 1$ for all $|s| \le \ell$. $\square$

Lemma 7.6 says that a membrane cannot bend more sharply than its own thickness. It is the statement a blow-up argument would otherwise have to assume, and here it is a property of the object.

Theorem 7.7. *Along a constrained gradient flow of a nondegenerate slab of half-thickness at least ℓ,*

$$\left|2\int_0^T\int_{\Sigma(t)} Kv^2\,\mathrm{d}A\,\mathrm{d}t\right| \le \frac{2\big(\mathcal{W}(0) - \mathcal{W}(T)\big)}{\ell^2} \le \frac{2\,\mathcal{W}(0)}{\ell^2}.$$

Proof. Bound $|K|$ by Lemma 7.6 and the remaining $\iint v^2$ by Proposition 7.2. $\square$

Theorem 7.7 takes K in L^∞ and v^2 in L^1, which is one end of a family. The other end is available and is sharper exactly where this paper works. It asks for the normal speed in L^∞, and the slab supplies all of that but one term.

Lemma 7.8. *On a nondegenerate slab of half-thickness at least ℓ,*

$$\big|2H(H^2 - K)\big| \le \frac{8}{27\,\ell^3},$$

attained at $k_1 = 1/\ell$, $k_2 = -1/3\ell$. Along the flow of Definition 7.1 with $P = 1$ it follows that

$$\begin{aligned}\sup_{\Sigma} |v| \ &\le\ \sup_{\Sigma} |\Delta H| + \frac{8}{27\,\ell^3},\\ \int_0^T \|\Delta H\|_{L^2}^2 \,\mathrm{d}t \ &\le\ 2\big(\mathcal{W}(0) - \mathcal{W}(T)\big) \ +\ \frac{128}{729\,\ell^6}\int_0^T |\Sigma(t)|\,\mathrm{d}t.\end{aligned}$$

Proof. In principal curvatures $2H(H^2 - K) = \frac{1}{4}(k_1 + k_2)(k_1 - k_2)^2$. Every interior critical point of that on the box $|k_i| \le 1/\ell$ has $k_1 = k_2$, where it vanishes, so its maximum lies on the boundary, and there it is $\frac{1}{4}(1+t)(1-t)^2\ell^{-3}$ over $t \in [-1, 1]$, maximised at $t = -1/3$ with value $\frac{8}{27}\ell^{-3}$. Lemma 7.6 puts the curvatures in that box. For the second statement, Definition 7.1 gives $\Delta H = -v - 2H(H^2 - K)$; take suprema for the first and L^2 norms for the second, using $(a+b)^2 \le 2a^2 + 2b^2$ and Proposition 7.2. $\square$

The area in Lemma 7.8 follows from the constraints: Proposition 7.15 inverts to $|\Sigma| = \big(V - \frac{4}{3}\pi\ell^3\chi\big)/2\ell$ at fixed enclosed volume, which Definition 7.1 fixes. For $P \ne 1$ the same statements hold with $\lambda_0 + \lambda_1 H + \lambda_2 K$ added to ΔH, where the multipliers are the coordinates of $(1-P)\delta\mathcal{W}$ in the basis of Proposition 7.17; the slab bounds H and K, and the multipliers are bounded by $\|\delta\mathcal{W}\|_{L^2}$ through the inverse Gram matrix of that basis, which is invertible away from the degeneracy noted after Proposition 7.17.

Proposition 7.9. *Along the same pathway,*

$$\begin{aligned}\left|2\int_0^T\!\!\int_{\Sigma(t)} K v^2 \,\mathrm{d}A\,\mathrm{d}t\right| \ &\le\ 2\,\sup|v|^2 \int_0^T \big(2\mathcal{W}(t) - 2\pi\chi(t)\big)\,\mathrm{d}t\\ &\le\ 2\Big(\sup|\Delta H| + \tfrac{8}{27\ell^3}\Big)^2 \int_0^T \big(2\mathcal{W} - 2\pi\chi\big)\,\mathrm{d}t.\end{aligned}$$

Proof. $|K| = |k_1 k_2| \le \frac{1}{2}(k_1^2 + k_2^2) = \frac{1}{2}|h|^2$ pointwise, so $\int |K|\,\mathrm{d}A \le \frac{1}{2}\mathcal{E} = 2\mathcal{W} - 2\pi\chi$ by Lemma 7.19. Pair that against $\sup|v|^2$ and apply Lemma 7.8. $\square$

Each of the two is sharper in a different regime. On a catenoid neck of waist c the total absolute curvature is $4\pi\tanh\xi$, independent of c, while $\sup|K| = c^{-2}$, so the ratio of the two bounds grows without limit as the neck closes: curvature concentrates, and an L^∞ norm is blind to a large value on a small set. On a sphere the two differ by the area alone. Theorem 7.7 needs a curvature ceiling, which Lemma 7.6 supplies from the leaflet separation; Proposition 7.9 needs $\sup|\Delta H|$, which the rest of this subsection supplies. Each closes the gap the other leaves.

What Lemma 7.8 leaves is reached by differentiating the dissipation identity once more. The terms that appear are bounded by a ladder whose rungs the slab and Lemma 7.8 already supply.

Proposition 7.10. *Write $\Lambda = \|\Delta H\|_{L^2(\Sigma)}$. On a nondegenerate slab of half-thickness at least ℓ,*

$$\begin{aligned}
\|\nabla H\|_{L^2}^2 \;&\le\; \ell^{-1}|\Sigma|^{1/2}\,\Lambda,\\
\|\nabla^2 H\|_{L^2}^2 \;&=\; \Lambda^2 - \int_\Sigma K|\nabla H|^2\,\mathrm{d}A \;\le\; \Lambda^2 + \ell^{-2}\|\nabla H\|_{L^2}^2,\\
\|\nabla H\|_{L^4}^2 \;&\le\; \frac{1}{\sqrt{\pi}}\big(\|\nabla H\|_{L^2}\|\nabla^2 H\|_{L^2} + \ell^{-1}\|\nabla H\|_{L^2}^2\big),\\
\|\nabla h\|_{L^2}^2 \;&=\; 4\|\nabla H\|_{L^2}^2 - 2\int_\Sigma H\,\mathrm{tr}\,h^3\,\mathrm{d}A + \int_\Sigma |h|^4\,\mathrm{d}A \;\le\; 4\|\nabla H\|_{L^2}^2 + \frac{8\,|\Sigma|}{\ell^4}.
\end{aligned}$$

Proof. The first is $\int|\nabla H|^2 = -\int H\Delta H$ on a closed surface with $\sup|H| < \ell^{-1}$ by Lemma 7.6. The second is Bochner's identity in two dimensions, where the Ricci curvature is Kg, with $\sup|K| < \ell^{-2}$. The third is the Ladyzhenskaya interpolation, run through the sharp Michael–Simon Sobolev inequality

$$2\sqrt{\pi}\Big(\int_\Sigma f^2\,\mathrm{d}A\Big)^{1/2} \;\le\; \int_\Sigma \sqrt{|\nabla f|^2 + 4f^2H^2}\,\mathrm{d}A, \tag{22}$$

where $2|H|$ is the length of the mean curvature vector. It holds on a closed surface with the constant $n|B^n|^{1/n}$ at $n=2$ [Bre21, Cor. 2], and in codimension one because that corollary is stated in $\mathbb{R}^{n+2}$ and a surface in $\mathbb{R}^3$ is one in $\mathbb{R}^4$. Take $f = |\nabla H|^2 + \varepsilon$ and let $\varepsilon \to 0$: the square root is at most $|\nabla f| + 2f|H|$, while $|\nabla|\nabla H|^2| \le 2|\nabla H||\nabla^2 H|$ by Cauchy–Schwarz on the contracted index and $|H| < \ell^{-1}$. The fourth is Simons' identity $\Delta h_{ij} = \nabla_i\nabla_j(2H) + 2Hh_{ik}h^k{}_j - |h|^2h_{ij}$, paired with h^{ij} and integrated: the leading term is $2\int h^{ij}\nabla_i\nabla_j H = -4\int|\nabla H|^2$ by Codazzi's $\nabla^j h_{ji} = 2\nabla_i H$, and $2|H||\,\mathrm{tr}\,h^3| + |h|^4 \le 8\ell^{-4}$ pointwise on the box of Lemma 7.6, attained at an umbilic corner. ☐

The fourth rung reaches the whole second fundamental form and not its trace. In two dimensions the two are independent: $\nabla(2K) = 8H\nabla H - 2h^{jk}\nabla_i h_{jk}$, and the trace-free part of ∇h is unconstrained by ∇H, so no bound of the form $|\nabla K| \le C|\nabla H|$ holds. The ladder terminates all the same: its top rung asks for nothing above ΔH, which Lemma 7.8 bounds in L^2 of spacetime.

Proposition 7.11. *The linearisation of $\delta\mathcal{W}$ in the normal direction v is $L[v] = \frac{1}{2}\Delta^2 v + a^{ij}\nabla_i\nabla_j v + b^k\nabla_k v + cv$ with*

$$\begin{aligned}
a^{ij} \;&=\; (H^2 - 2K)\,g^{ij} \;+\; 2Hh^{ij},\\
b^k \;&=\; 6H\nabla^k H \;+\; 2h^{kj}\nabla_j H \;-\; 2\nabla^k K,\\
c \;&=\; 4H\Delta H + 2h^{ij}\nabla_i\nabla_j H - \Delta K + 6|\nabla H|^2 + 12H^4 - 14H^2K + 2K^2.
\end{aligned}$$

On a nondegenerate slab of half-thickness at least ℓ the coefficients obey

$$|a| \;\le\; \frac{2}{\ell^2}, \qquad |b| \;\le\; \frac{C\,|\nabla h|}{\ell}, \qquad |c| \;\le\; C\Big(\frac{|\nabla^2 H|}{\ell} + |\nabla h|^2 + \frac{1}{\ell^4}\Big),$$

the first two attained at $k_1 = -k_2 = \ell^{-1}$.

Proof. Under a normal motion $\delta g_{ij} = -2vh_{ij}$ and $\delta h_{ij} = \nabla_i\nabla_j v - vh_{ik}h^k{}_j$, whose trace is the second half of Eq. (20). These give $\delta K = 2H\Delta v - h^{ij}\nabla_i\nabla_j v + 2HKv$ and, through $\delta\Gamma$ and Codazzi, $\delta(\Delta f) = 2vh^{ij}\nabla_i\nabla_j f + \langle 2h(\nabla v) - 2H\nabla v + 2v\nabla H, \nabla f\rangle$. Apply both to $\delta\mathcal{W} = \Delta H + 2H(H^2 - K)$ and collect by the order of the derivative falling on v. For the bounds, a is diagonal in principal directions with entries $H^2-2K+2Hk_i$, whose modulus is at most $2\ell^{-2}$ on the box of Lemma 7.6; b is a curvature against a first derivative of curvature, and ∇K is one by $\nabla(2K) = 8H\nabla H - 2h^{jk}\nabla h_{jk}$; and ΔK contains $|\nabla h|^2$ by the same identity differentiated once more. □

Corollary 7.12. *On the round sphere of radius r, $b = c = 0$ and $L = \frac{1}{2}\Delta^2 + r^{-2}\Delta$. Its eigenvalue on the k-th spherical harmonic is $\frac{1}{2}\lambda_k(\lambda_k - 2r^{-2})$ with $\lambda_k = k(k+1)r^{-2}$, which vanishes exactly at $k \in \{0,1\}$ and is positive thereafter.*

Proof. The sphere is umbilic, so every derivative of curvature vanishes and the quartic $12H^4 - 14H^2K + 2K^2$ vanishes at $H^2 = K$; a collapses to $r^{-2}g$. □

The kernel in Corollary 7.12 is four-dimensional, spanned by the constant and the three linear spherical harmonics, and it is the tangent space at Σ to the four-parameter family of round spheres: one dilation and three translations, both of which leave $\mathcal{W}$ at 4π. That is the check on c. Any error in it moves the eigenvalue at $k = 1$ off zero and puts a translation outside the kernel.

Proposition 7.13. *Along the flow of Definition 7.1 with $P = 1$,*

$$\frac{\mathrm{d}^2}{\mathrm{d}t^2}\mathcal{W} \;=\; 2\int_\Sigma v\,L[v]\,\mathrm{d}A \;+\; 2\int_\Sigma Hv^3\,\mathrm{d}A,$$

where L is the operator of Proposition 7.11, and

$$\int_0^T \|\Delta v\|_{L^2}^2\,\mathrm{d}t \;\le\; C\big(\ell, |\Sigma|, \mathcal{W}(0), \|v(0)\|_{L^2}\big),$$

so that $\int_0^T \sup_\Sigma |v|^2\,\mathrm{d}t < \infty$.

Proof. $\mathrm{d}\mathcal{W}/\mathrm{d}t = -\int v^2\,\mathrm{d}A$ and $\partial_t(\mathrm{d}A) = -2Hv\,\mathrm{d}A$ by Eq. (20), so differentiating again gives $-2\int v\,\partial_t v + 2\int Hv^3$, and $\partial_t v = -L[v]$. Integrating in time, $\int_0^T 2\int vL[v] = \|v(0)\|_{L^2}^2 - \|v(T)\|_{L^2}^2 - 2\int_0^T\int Hv^3$. The principal part contributes $\int(\Delta v)^2$ after two integrations by parts. Of the rest, $|\int v\,a\nabla^2 v| \le 2\ell^{-2}\|v\|_{L^2}\|\nabla^2 v\|_{L^2}$ with $\|\nabla^2 v\|_{L^2}^2 \le \|\Delta v\|_{L^2}^2 + \ell^{-2}\|\nabla v\|_{L^2}^2$ by Bochner; $|\int v\,b\cdot\nabla v| \le \|b\|_{L^2}\|v\|_{L^4}\|\nabla v\|_{L^4}$ with $\|b\|_{L^2} \le C\ell^{-1}\|\nabla h\|_{L^2}$, which is the fourth rung of Proposition 7.10; and the term of c containing ΔK moves both derivatives onto v^2, since $\int(\Delta K)v^2 = \int K\,\Delta(v^2) = 2\int K\big(v\Delta v + |\nabla v|^2\big)$, which Lemma 7.6 bounds and which removes $|\nabla h|^2$ from the estimate altogether. The remaining terms of c pair $\|\Delta H\|_{L^2}$,

$\|\nabla^2 H\|_{L^2}$ and $\|\nabla H\|_{L^4}^2$ against $\|v\|_{L^4}^2$, all rungs of Proposition 7.10. Finally $|\int Hv^3| \leq \ell^{-1}\|v\|_{L^2}\|v\|_{L^4}^2$ with $\|v\|_{L^4}^2 \leq \pi^{-1/2}(\|v\|_{L^2}\|\nabla v\|_{L^2} + \ell^{-1}\|v\|_{L^2}^2)$, which is Eq. (22) at $f = v^2 + \varepsilon$, and $\|\nabla v\|_{L^2}^2 \leq \|v\|_{L^2}\|\Delta v\|_{L^2}$. Young's inequality puts each under any prescribed fraction of $\|\Delta v\|_{L^2}^2$, and Proposition 7.2 bounds $\|v\|_{L^2}$. The last statement is the Sobolev embedding $H^2(\Sigma) \hookrightarrow C^0(\Sigma)$ in two dimensions. □

Every coefficient in Proposition 7.13 is bounded by Lemma 7.6 and Proposition 7.10, so the estimate rests on the slab and on the flow. The one quantity it takes from outside is the constant of Eq. (22), which is $2\sqrt{\pi}$ and is sharp, attained on the flat disc and on nothing else [Bre21, Thm. 3]. With it, Proposition 7.9 closes.

Corollary 7.14.

$$\left|2\int_0^T\int_{\Sigma(t)} Kv^2\,\mathrm{d}A\,\mathrm{d}t\right| \;\leq\; 2\big(2\mathcal{W}(0) - 2\pi\min_t \chi(t)\big)\int_0^T \sup_{\Sigma(t)}|v|^2\,\mathrm{d}t,$$

and the right side is finite by Proposition 7.13.

The supremum belongs inside the time integral, which is all Proposition 7.9 ever needed and is strictly less than a supremum over spacetime. That is where the gap was: Proposition 7.2 controls v in L^2 of spacetime and never in L_t^∞, so a bound written with $\sup_t$ rests on more than the flow supplies.

The asymmetry follows from which norms the flow supplies. Hölder at conjugate exponents bounds the correction by $\|K\|_{L^p}\|v\|_{L^{2p'}}^2$, and the curvature side is available at every p, since $|K|^p \leq \|K\|_\infty^{p-1}|K|$ pointwise gives $\|K\|_{L^p} \leq \ell^{-2(1-1/p)}(2\mathcal{W} - 2\pi\chi)^{1/p}$, interpolating Lemma 7.6 at $p = \infty$ with Proposition 7.9 at $p = 1$. The speed side is available at $p = \infty$ alone, since $\|v\|_{L^2}$ over spacetime is what Proposition 7.2 supplies and every finite p asks for a higher norm. The family therefore has one computable member, which is Theorem 7.7, and Proposition 7.9 complements it without improving on it. What Corollary 7.14 changes is a different thing: it removes the supremum over spacetime, which is the one quantity the flow never controls, and leaves the second member conditional on the form of L alone.

A neck of waist radius c has $|k| = 1/c$ there, so a nondegenerate slab requires $c > \ell$: the neck cannot close, and a pathway must be cut at the leaflet separation. The embeddedness condition of the rim in Section 4 floors a pore at the same length, so one cutoff serves both.

Proposition 7.15. *The slab has volume $V = 2\ell A + \frac{4}{3}\pi\ell^3\chi(\Sigma)$. At fixed V and fixed ℓ a surgery changes the area by $\Delta A = -\frac{2}{3}\pi\ell^2\,\Delta\chi$.*

Proof. Integrate the area factor of Lemma 7.6 over $s \in [-\ell, \ell]$. The term linear in s is odd and drops, leaving $2\ell + \frac{2}{3}\ell^3 K$ pointwise, and $\mu(\Sigma) = 2\pi\chi$. □

A surgery therefore changes the area by a definite amount, set by the thickness alone: at $\ell = 1.5\,\mathrm{nm}$ a pinch moves $4\pi\ell^2/3 \approx 9.4\,\mathrm{nm}^2$, some twenty-six lipid head groups. A surface model cannot see this, the shift vanishing with ℓ.

Corollary 7.16. *The two leaflets differ in area by* $A_+ - A_- = -4\ell \int_\Sigma H\,\mathrm{d}A$.

Proof. Subtract the two area elements $\big(1 \mp 2H\ell + K\ell^2\big)\,\mathrm{d}A$ and integrate. □

Corollary 7.16 is the relation on which area-difference elasticity is built [Mia+94, Eq. 2.4], obtained here from Lemma 7.6. Its left side counts lipids and its right side is a geometric invariant of the mid-surface, and ℓ converts one into the other.

Proposition 7.17. *Under a normal motion of a closed surface,*

$$\delta \int_\Sigma \mathrm{d}A \;=\; -\int_\Sigma 2Hv\,\mathrm{d}A, \qquad \delta \int_\Sigma H\,\mathrm{d}A \;=\; -\int_\Sigma Kv\,\mathrm{d}A,$$

and $\delta\,\mathrm{vol} = \int_\Sigma v\,\mathrm{d}A$. *The three constrained quantities are therefore conjugate to* 1, $2H$ *and* K.

Proof. The first and third are Eq. (20) and the divergence theorem. For the second, Eq. (20) gives $\partial_t(H\,\mathrm{d}A) = \big(\tfrac{1}{2}\Delta v + (\tfrac{1}{2}|h|^2 - 2H^2)v\big)\,\mathrm{d}A$, and $\tfrac{1}{2}|h|^2 - 2H^2 = -K$ in two dimensions, while $\int \Delta v\,\mathrm{d}A = 0$. □

Lipids do not exchange between leaflets on the timescale of a pathway, so $A_+ - A_-$ is fixed, so $\int H\,\mathrm{d}A$ is fixed by Corollary 7.16. The three constraints of Definition 7.1 are thus conjugate to 1, H and K, and they span a three-dimensional subspace except where K is an affine function of H pointwise. Spheres, cylinders and tori of revolution all satisfy such a relation, so the degeneracy is common.

7.4. **Total squared curvature and the confinement of events.**

Definition 7.18. The *total squared curvature* of a configuration is $\mathcal{E}(\Sigma) = \int_\Sigma |h|^2\,\mathrm{d}A$.

Lemma 7.19. $\mathcal{E} = 4\mathcal{W} - 4\pi\chi$, *it is invariant under* $\Sigma \mapsto \mu\Sigma$, *and* $\mathcal{E} \geq 2\mathcal{W} \geq 8\pi m$ *for a configuration of* m *components.*

Proof. $|h|^2 = 4H^2 - 2K$ and $\mu(\Sigma) = 2\pi\chi$ by Definition 4.4, which is what the second term means at a configuration with joins. Both terms are scale invariant. Pointwise $k_1^2 + k_2^2 \geq \tfrac{1}{2}(k_1 + k_2)^2$, and $\mathcal{W} \geq 4\pi$ on each closed component [Wil65]. □

Scale invariance is what a blow-up argument requires of $\mathcal{E}$, and neither the area nor the enclosed volume has it. A catenoid of any waist has $\mathcal{E} = 8\pi$, and the part of it within half-height ξc has $8\pi\tanh\xi$, the same function of the same neck parameter that governs the saddle-splay accrual and the bending energy of the capped neck. A pinching neck therefore concentrates 8π of $\mathcal{E}$ into a ball of shrinking radius, and by Lemma 7.6 it stops short of doing so.

Theorem 7.20. *Let $\mathcal{W}$ be nonincreasing along a pathway. Every surgery occurs at a time in $\{t : \mathcal{W}(t) \geq 8\pi\}$, which is an initial interval. Once the energy falls below 8π the diffeomorphism type of $\Sigma(t)$ is constant, and below $2\pi^2$ every component is a sphere.*

Proof. A surgery passes through a configuration with a point of multiplicity two, where $\mathcal{W} \geq 8\pi$ [LY82, Thm. 6]. The limit configuration is not smooth, so the bound is applied to it in the setting of Definition 4.4, where Corollary 4.6 preserves the total mass through the degeneration and lower semicontinuity of $\mathcal{W}$ extends the inequality to the limit. A nonincreasing function is below 8π on a terminal interval. The second statement is the genus bound of [MN14]. □

Theorem 7.21. *Write $m(t)$ for the number of components. Then $m(t) \leq \mathcal{W}(0)/4\pi$ throughout. A pathway on which no component splits performs at most $m(0) - 1 \leq \mathcal{W}(0)/4\pi - 1$ merges, and a pathway on which none merge performs at most $\mathcal{W}(0)/4\pi - m(0)$ splits. A pathway with both satisfies only the difference of the two numbers.*

Proof. The first is Lemma 7.19. A merge lowers m by one and $m \geq 1$, which gives the second. A split raises m by one and lowers $\mathcal{E}$ by 8π, since χ rises by 2 while $\mathcal{W}$ is continuous across the cut, so n splits require $\mathcal{E}(0) - 8\pi n \geq 8\pi(m(0) + n)$ by Lemma 7.19; with $\chi(0) = 2m(0)$ that is the third. A merge raises $\mathcal{E}$ by 8π and a split restores a component, so an interleaved pathway satisfies $m(0) - 1 \geq \#\text{merges} - \#\text{splits}$ and no more. □

Both bounds are attained. For k round vesicles $\mathcal{W}(0) = 4\pi k$ and Theorem 7.21 returns exactly the $k - 1$ merges they need; for one round sphere it returns no splits, and for a dumbbell at $\mathcal{W} = 8\pi$ exactly one.

Remark 7.22. Theorem 7.20 and Theorem 7.21 need only that $\mathcal{W}$ is nonincreasing, which Proposition 7.2 supplies for any number of constraints. An external force f not derived from the energy gives $\mathrm{d}\mathcal{W}/\,\mathrm{d}t = -\|P\delta\mathcal{W}\|^2 + \langle \delta\mathcal{W}, f\rangle$, and for $f = 2\,\delta\mathcal{W}$ that is $\|P\delta\mathcal{W}\|^2 + 2\|(1 - P)\delta\mathcal{W}\|^2 > 0$. A membrane that fuses more often than Theorem 7.21 allows is therefore being driven, and the work done on it is at least $4\pi\kappa_m$ per event beyond the bound.

7.5. **Minimisers and the flow.** The same threshold appears throughout the literature. Three numbers order the Willmore energy of a closed surface, and each is attained: 4π at the round sphere and nowhere else [Wil65], $2\pi^2$ at the Clifford torus and nowhere else in positive genus [MN14], and 8π as a floor at any point of multiplicity two [LY82, Thm. 6]. They are distinct and in that order, $4\pi < 2\pi^2 < 8\pi$.

The genus-one minimum sits below the threshold. A torus can therefore exist at energies at which Theorem 7.20 forbids any event, so the threshold is a statement about events and not about genus: it bounds when the type may change, never which types occur. That is the sense in which Δ and $\mathcal{W}$ are independent coordinates, as Corollary 6.3 has it for Δ and the energy.

The same number arrives from the evolution. The Willmore flow from initial data of small energy exists for all time and converges to a round sphere [KS01], and the threshold for that is 8π, since the only Willmore spheres below 8π in energy are the round ones [Bry84]. A surface below 8π therefore flows to a sphere without changing type, which is Theorem 7.20 read forwards in time. The static route through [LY82] and the dynamic route through [KS01] give the same 8π, and Theorem 7.21 is the counting form of it.

The constrained problem is settled at every genus. At fixed isoperimetric ratio a minimiser of sphere type exists at every ratio [Sch12]; at genus $\mathrm{g} \geq 1$ one exists at every ratio at which the constrained infimum lies below 8π [KMR14, Thm. 1.2]; and that condition holds at every genus and every ratio in $(0, 1)$, by a comparison surface built from catenoidal bridges over a solution of the linearised Willmore equation [KM21, Thm. 1.2]. Under the constraints of Definition 7.1 the matching statement is available at fixed area and fixed total mean curvature [SW25, Thm. 1.1], which by Corollary 7.16 is fixed area difference, and for the full Eq. (12) at sphere type [MS20]. For the constrained gradient flow of Eq. (12), global existence and convergence are proved below computed energy thresholds [RSS24]. The threshold in every one of these is 8π, which is Theorem 7.20's. Each fixes the topology. A pathway does not, and Section 8 returns to what that leaves open.

7.6. **Cost of a cut.** Section 5 splits the surgery number between the classes and Section 6 gives its energy. One number is left, and Theorem 7.21 is finite as soon as it is positive.

Proposition 7.23. *Let $t_1 < \cdots < t_N$ be the event times of a pathway along which $\mathcal{W}$ is nonincreasing, and suppose $\mathcal{W}(t_i) - \mathcal{W}(t_{i+1}) \geq \eta > 0$ for each i. Then*

$$N \;\leq\; 1 + \frac{\mathcal{W}(0) - 8\pi}{\eta}.$$

Proof. Every t_i lies in $\{\mathcal{W} \geq 8\pi\}$ by Theorem 7.20, so the $N-1$ drops sum to at most $\mathcal{W}(t_1) - \mathcal{W}(t_N) \leq \mathcal{W}(0) - 8\pi$. □

The interleaved case, which Theorem 7.21 constrains only through the difference of the two counts, therefore needs a floor on the dissipation between consecutive events. The slab supplies one. A pathway on a nondegenerate slab never pinches, since Lemma 7.6 floors every neck at ℓ, so an event is a cut made at a finite scale, and not a singularity of the flow. The energy a cut dissipates is computable.

Write $\kappa[\gamma] = \oint_\gamma k_g \, \mathrm{d}s$ for the total geodesic curvature of a seam, taken with the conormal pointing into the region named.

Lemma 7.24. *Let $D \subset \Sigma$ be a disc. Then*

$$\mathcal{W}(D) \;\geq\; 2\pi - \kappa[\partial D],$$

with equality exactly when D is umbilic. The flat disc and every spherical cap attain it.

Proof. $H^2 - K = \big(\tfrac{1}{2}(k_1 - k_2)\big)^2 \geq 0$ pointwise, so $\mathcal{W}(D) \geq \int_D K\,\mathrm{d}A$, and Gauss–Bonnet on a disc gives $\int_D K\,\mathrm{d}A = 2\pi\chi(D) - \kappa[\partial D]$ with $\chi(D) = 1$. Equality forces $k_1 = k_2$ throughout. On a sphere of radius a the cap of polar half-angle θ has $\mathcal{W} = 2\pi(1 - \cos\theta)$ against a seam of $2\pi\cos\theta$, which sum to 2π at every θ; the seam is a geodesic at $\theta = \pi/2$ alone, and the flat disc has nothing against a seam of 2π. $\square$

A seam term is constrained by what the merge puts on the other side of it, and the two seams of a merge bound the tube.

Lemma 7.25. *Form Σ' from Σ by removing two discs $D_\pm$ and gluing an annulus N along $\partial D_+ \cup \partial D_-$, with Σ' of class C^1 across both seams. Then*

$$\kappa[\partial D_+] + \kappa[\partial D_-] \;=\; -\int_N K\,\mathrm{d}A.$$

Proof. Write $\Sigma_r = \Sigma \setminus (D_+ \cup D_-)$, the part both surfaces retain. Along either seam the tangent plane of N agrees with that of Σ_r, and so with that of the disc removed, since both surfaces are C^1 there, so a seam has one geodesic curvature up to the conormal. The annulus occupies the side of the seam its disc vacated, which is the side away from Σ_r, so the conormal into N is the conormal into that disc, with the same sign. Gauss–Bonnet on N reads $\int_N K\,\mathrm{d}A + \kappa[\partial N] = 2\pi\chi(N) = 0$, and $\kappa[\partial N]$ is the sum above. $\square$

A pore fixes the sign, both of its terms being elementary. Its two removed discs are flat, so each seam term is 2π by Gauss–Bonnet and their sum is 4π, while the rim it glues in has $\int_N K\,\mathrm{d}A = -4\pi$ by Lemma 4.1, whatever its profile and radii. A cut whose seams are geodesics into a tube of vanishing Gaussian curvature reports nothing here, both sides being zero.

Theorem 7.26. *Let a merge remove two discs $D_\pm \subset \Sigma$ and glue in a tube N as in Lemma 7.25. Then*

$$\mathcal{W}(\Sigma) - \mathcal{W}(\Sigma') \;\geq\; 4\pi - \int_N \big(H^2 - K\big)\,\mathrm{d}A,$$

an equality when both discs are umbilic. The integrand is nonnegative, so the drop never exceeds 4π; it exceeds $4\pi - |N|/\ell^2$, and so is positive whenever the tube has area below $4\pi\ell^2$.

Proof. $\mathcal{W}(\Sigma) - \mathcal{W}(\Sigma') = \mathcal{W}(D_+) + \mathcal{W}(D_-) - \mathcal{W}(N)$, each disc obeys Lemma 7.24, and Lemma 7.25 moves the two seam terms onto the tube, where they join $\mathcal{W}(N)$ as the single integrand $H^2 - K$. That integrand is $\big(\tfrac{1}{2}(k_1 - k_2)\big)^2$, which is half the squared trace-free second fundamental form and is at most ℓ^{-2} on the box of Lemma 7.6, attained at $k_1 = -k_2 = \ell^{-1}$. For sharpness, two round vesicles of radius c joined along their equators by a cylinder of radius c and length L have $4\pi + \pi L/2c$ against the 8π they had apart, a drop of $4\pi - \pi L/2c$ which is the bound exactly, the caps being umbilic, and which reaches 4π as the two touch. $\square$

Writing $\mathring{h} = h - Hg$ for the trace-free part of the second fundamental form, $H^2 - K = \frac{1}{2}|\mathring{h}|^2$, and $\int |\mathring{h}|^2$ is invariant under conformal maps of the ambient space. Seams that are geodesics give $\int_N K\,\mathrm{d}A = 0$ and return $4\pi - \mathcal{W}(N)$, so the general form contains that one and sharpens it, the tube's Willmore energy giving way to its conformally invariant part. At $\ell = 1.4\,\mathrm{nm}$ the area condition is a tube below $24.6\,\mathrm{nm}^2$, which at radius ℓ is a length below $2.8\,\mathrm{nm}$, and a fusion stalk is that object.

Corollary 7.27. *The pore of Theorem 4.2 attains Theorem 7.26, and the value attained is $-\mathcal{W}(N)$, the bending part of Eq.* (15) *divided by 2κ. A pore costs bending energy and releases none.*

Proof. The two discs a pore removes are flat, hence umbilic, which is the equality case of Lemma 7.24, and each has a seam term of 2π. Its rim has $\int_N K\,\mathrm{d}A = -4\pi$ by Lemma 4.1 whatever its profile and radii, which is $-(2\pi + 2\pi)$ as Lemma 7.25 requires. The floor is then $4\pi - \big(\mathcal{W}(N) + 4\pi\big) = -\mathcal{W}(N)$, and $\mathcal{W}(D_+) + \mathcal{W}(D_-) - \mathcal{W}(N) = -\mathcal{W}(N)$ is the change itself. $\square$

At the aspect ratio ρ^* of Corollary 6.5 that is -1.895, so a released rim costs 3.79κ in bending, which is Corollary 6.5 reached along a second route.

A minimal tube shows how much the seams can contribute. A catenoid has $H \equiv 0$ and $K < 0$ everywhere, so a catenoidal neck of waist a and half-height w has $\int_N K\,\mathrm{d}A = -4\pi\tanh(w/a)$, its seams contribute $4\pi\tanh(w/a)$ between them, and the floor is $4\pi\big(1 - \tanh(w/a)\big)$: positive at every finite length and decaying as the neck draws out. That the seam sum is nonzero is exactly what stops a catenoidal neck from meeting both its seams as geodesics, so a hypothesis of a geodesic cut would exclude the minimal tube outright. The floor 4π is the constant in the connected-sum inequality $\mathcal{W}(\Sigma_1 \# \Sigma_2) < \mathcal{W}(\Sigma_1) + \mathcal{W}(\Sigma_2) - 4\pi$ [SW25, Thm. 1.2], strict there because the round sphere is excluded and attained here because it is not.

The same family settles the area threshold of Theorem 7.26 in terms of the rims alone. Write $\xi = w/a$ for the neck parameter, as elsewhere in this section.

Corollary 7.28. *A catenoidal tube of waist a and half-height w spans two coaxial circles of radius $r = a\cosh\xi$, and*

$$|N| \;\le\; 2\xi_*\,\pi r^2 \;=\; 2.39936\,\pi r^2, \qquad \xi_*\tanh\xi_* = 1,$$

with equality exactly at $\xi = \xi_* = 1.19968\ldots$. The drop of Theorem 7.26 is therefore positive for every catenoidal tube whose rims satisfy $r < \ell\sqrt{2/\xi_*} = 1.29117\,\ell$, whatever its length.

Proof. The tube has area $\pi a^2(2\xi + \sinh 2\xi)$ and rim radius $a\cosh\xi$, so

$$\frac{|N|}{\pi r^2} \;=\; \frac{2\xi + \sinh 2\xi}{\cosh^2\xi} \;=\; 2\xi\,\mathrm{sech}^2\,\xi + 2\tanh\xi,$$

whose derivative is $4\operatorname{sech}^2\xi\,(1-\xi\tanh\xi)$. The factor $\xi\tanh\xi$ is a product of positive increasing functions, so it meets 1 once, the derivative changes sign once, and the ratio has a single maximum, at ξ_*. There $\tanh\xi_* = 1/\xi_*$ and $\operatorname{sech}^2\xi_* = 1-\xi_*^{-2}$, so the ratio collapses to $2\xi_*$. The second statement is $2\xi_*\pi r^2 < 4\pi\ell^2$ against Theorem 7.26. □

The extremal tube is the longest one that exists. The same ξ_* is where $w/r = \xi\operatorname{sech}\xi$ is stationary, which is the classical fold beyond which no catenoid spans a given pair of rings, so the case deciding the threshold is the limiting member of the family and not an interior one.

The hypothesis of the next theorem should be read against that. Theorem 7.26 returns 4π only where the tube's trace-free curvature integrates to nothing, which on an annulus is the vanishing tube of the family above, and the integrand $\big(\frac{1}{2}(k_1-k_2)\big)^2$ is largest exactly at $k_1=-k_2$, the shape a neck takes. A stalk at the area threshold above leaves little of the floor. What follows therefore describes pathways whose necks are small against ℓ, and Proposition 7.23 is what a smaller η leaves.

Theorem 7.29. *Along a pathway on which $\mathcal{W}$ is nonincreasing and every merge meets Theorem 7.26 with $\eta \geq 4\pi$, the total number of events is at most*

$$\frac{\mathcal{E}(0)-8\pi}{8\pi} = \frac{\mathcal{W}(0)}{2\pi} - \frac{\chi(0)}{2} - 1,$$

and this is attained: k round vesicles give exactly $k-1$.

Proof. $\mathcal{E} = 4\mathcal{W} - 4\pi\chi$ by Lemma 7.19, so an event changes it by $4\Delta\mathcal{W} - 4\pi\Delta\chi$. A split raises χ by 2 and cannot raise $\mathcal{W}$, so it lowers $\mathcal{E}$ by at least 8π; a merge lowers χ by 2 and lowers $\mathcal{W}$ by at least 4π, so it lowers $\mathcal{E}$ by at least 8π as well, the topological gain being cancelled exactly. Between events χ is constant and $\mathcal{W}$ nonincreasing, so $\mathcal{E}$ is nonincreasing there too, and $\mathcal{E} \geq 8\pi$ throughout by Lemma 7.19. For k round vesicles $\mathcal{E}(0) = 8\pi k$. □

The split needs no floor of its own. It is the merge that pays, and it pays exactly enough: at $\eta = 4\pi$ the 8π a merge gains in $\mathcal{E}$ by lowering χ is spent in full on the bending energy, so both kinds of event spend from the same $\mathcal{E}$ and the interleaved case is bounded by the same number as either pure case. Below $\eta = 2\pi$ that cancellation fails, a merge returns $\mathcal{E}$ to the pathway, and the two counts have to be bounded separately: Proposition 7.23 for the merges and Lemma 7.19 for the splits.

8. Limits

8.1. **Failure of the partition.** A surgery merging components of different classes admits no consistent class assignment, the resulting component being required to inherit both. Δ therefore has no value after such an event. This is rupture, and it separates the fusion route from the failure route. The separation rests on the partition and not on χ, and so is insensitive to tilt of any magnitude by Proposition 3.1.

The two components need not belong to different membranes. When they are the proximal and distal leaflets of one bilayer, the event is that bilayer fusing with itself: the sheet it produces is again unstable, and the pore nucleated inside that sheet opens the membrane to its own exterior, destroying it. Assumption 2.2 excludes this by hypothesis, and nothing in the construction excludes it otherwise.

8.2. **Three leaflets at one stratum.** The partition is a two-colouring, and three components meeting along a common stratum admit no injective assignment of two classes. The outer rim of a hemifusion diaphragm is where three bilayers meet, and would be such a stratum at the bilayer level. Under Assumption 2.2 the three monolayers passing that rim share no point, the pairwise intersections are empty, and inclusion and exclusion has nothing to subtract. The union's Euler characteristic is then the plain sum, and were the three to share a stratum it would differ by twice that stratum, so the assumption changes the answer and is visible in it.

8.3. **Variation of the modulus.** Every energy statement here reduces $\int \bar{\kappa} K \, \mathrm{d}A$ to $2\pi\bar{\kappa}\chi$, which requires $\bar{\kappa}$ outside the integral. Continuity suffices in the limit, the singular part of Eq. (4) taking the modulus's value on the set where Corollary 4.6 concentrates it. A modulus that jumps across the rim breaks that reduction: no single value then reproduces the two-valued weighting of Theorem 4.5, and the two ends of the family disagree. This is the undetermined constant of Section 6.3.

A modulus varying over the surface, and not across the rim, is a different object and is under active study. Raising $\bar{\kappa}$ from $-\kappa$ to nearly zero on the merging region alone, at $-\kappa$ elsewhere, takes a computed fusion barrier from $226\, k_B T$ [Bot+24, p. 2] to $16\, k_B T$ at $\kappa = 20\, k_B T$, and to $39\, k_B T$ at $\kappa = 50\, k_B T$ [Bot+24, p. 4]. The mechanism is the one this subsection names, stated from the other side: "k_G would go under the integral sign, loosening the Gauss–Bonnet theorem constraint" [Bot+24, p. 2]. Proposition 6.1 is exactly the statement that fails when it does, and $4\pi|\bar{\kappa}|$ is what a variable modulus puts in question. The value approached is "close to the stability limit with respect to saddle deformations" [Bot+24, p. 2], so such a variation runs to the edge of the same interval $(-1, 0)$ that Section 6.3 works in [She+06] and no further.

That variation is over position. Theorem 6.2 needs a different one, over class: the two leaflets taking $\bar{\kappa}_\mathrm{p} \neq \bar{\kappa}_\mathrm{d}$ at the same point of space. The two are independent, and only the second makes Δ visible in an energy.

8.4. **Scope.** The surgery number, the class imbalance, the parity and the rim's -4π are geometry and are exact. Converting a surgery into an energy runs through a modulus measured in flat and mesophase geometries, and Section 6.3 shows that neither quantity reported for a pore tests it. The floor of Theorem 7.26 asks of a merge that the glued surface be C^1 across both seams and that the tube be an annulus, which is what lowering χ by two amounts to; it asks nothing about where the cut is made.

Section 6.4 computes a barrier height for the open-pore branch. The leg from the intact membrane to the first rim runs through a state with a water wire and no rim at all [SAH25, pp. 3–4], which is where a nucleation free energy is reported and which no surface model reaches. That leg is the gap between an energy landscape and a nucleation theory, and it is molecular: tilt is the mode the measured barrier tracks [SAH25, Fig. 6g], and a surface has no coordinate for it. Everything this paper computes about a pore is therefore a statement about a state the membrane occupies after nucleating one, which is the right reading of $4\pi|\bar{\kappa}_m|$ as well.

Nothing here produces a minimiser or a flow. What Section 7.5 imports instead is an existence theory complete at every genus: minimisers of $\mathcal{W}$ at fixed isoperimetric ratio exist at genus zero [Sch12, Thm. 1.1], at genus $\mathrm{g} \geq 1$ below 8π [KMR14, Thm. 1.2], and therefore at every genus and every ratio [KM21, Thm. 1.2]. Two of the three constraints of Definition 7.1 are fixed area and fixed total mean curvature, and there a minimiser exists at every genus too [SW25, Thm. 1.1], while Eq. (12) itself has one at sphere type [MS20]. Each fixes the topology, and a pathway does not. What remains open is a variational principle selecting the pathway between two types. Theorem 7.29 bounds how many events such a principle may produce, and produces none of them.

References

[Bot+24] Matteo Bottacchiari, Mirko Gallo, Marco Bussoletti and Carlo Massimo Casciola. 'The local variation of the Gaussian modulus enables different pathways for fluid lipid vesicle fusion'. In: *Scientific Reports* 14 (2024), p. 23. DOI: 10.1038/s41598-023-50922-7.

[Bre21] Simon Brendle. 'The isoperimetric inequality for a minimal submanifold in Euclidean space'. In: *Journal of the American Mathematical Society* 34.2 (2021), pp. 595–603. DOI: 10.1090/jams/969. arXiv: 1907.09446 [math.DG].

[Bry84] Robert L. Bryant. 'A duality theorem for Willmore surfaces'. In: *Journal of Differential Geometry* 20.1 (1984), pp. 23–53. DOI: 10.4310/jdg/1214438991.

[CK03] Leonid V. Chernomordik and Michael M. Kozlov. 'Protein-lipid interplay in fusion and fission of biological membranes'. In: *Annual Review of Biochemistry* 72 (2003), pp. 175–207. DOI: 10.1146/annurev.biochem.72.121801.161504.

[CK08] Leonid V. Chernomordik and Michael M. Kozlov. 'Mechanics of membrane fusion'. In: *Nature Structural and Molecular Biology* 15 (2008), pp. 675–683.

[Des15] Markus Deserno. 'Fluid lipid membranes: from differential geometry to curvature stresses'. In: *Chemistry and Physics of Lipids* 185 (2015), pp. 11–45. DOI: 10.1016/j.chemphyslip.2014.05.001.

[GD26] Seamus F. Gallagher and Markus Deserno. 'Topological approach to measuring the Gaussian curvature modulus of lipid membranes in simulation'. In: *Physical Review Letters* 136.23 (2026). DOI: 10.1103/6d6f-q1mg.

[HBD12] Mingyang Hu, John J. Briguglio and Markus Deserno. 'Determining the Gaussian curvature modulus of lipid membranes in simulations'. In: *Biophysical Journal* 102 (2012), pp. 1403–1410.

[Hel73] W. Helfrich. 'Elastic properties of lipid bilayers: theory and possible experiments'. In: *Z. Naturforsch. C* 28 (1973), pp. 693–703.

[KCK02] Yonathan Kozlovsky, Leonid V. Chernomordik and Michael M. Kozlov. 'Lipid intermediates in membrane fusion: formation, structure, and decay of hemifusion diaphragm'. In: *Biophysical Journal* 83 (2002), pp. 2634–2651.

[KK02] Yonathan Kozlovsky and Michael M. Kozlov. 'Stalk model of membrane fusion: solution of energy crisis'. In: *Biophysical Journal* 82 (2002), pp. 882–895.

[KM21] Robert Kusner and Peter McGrath. *On the Canham problem: bending energy minimizers for any genus and isoperimetric ratio.* 2021. arXiv: 2104.10045 [math.DG].

[KMR14] Laura Gioia Andrea Keller, Andrea Mondino and Tristan Rivière. 'Embedded surfaces of arbitrary genus minimizing the Willmore energy under isoperimetric constraint'. In: *Archive for Rational Mechanics and Analysis* 212.2 (2014), pp. 645–682. DOI: 10.1007/s00205-013-0694-9.

[KS01] Ernst Kuwert and Reiner Schätzle. 'The Willmore flow with small initial energy'. In: *J. Differential Geom.* 57 (2001), pp. 409–441.

[LY82] Peter Li and Shing-Tung Yau. 'A new conformal invariant and its applications to the Willmore conjecture and the first eigenvalue of compact surfaces'. In: *Invent. Math.* 69 (1982), pp. 269–291.

[MA02] Vladislav S. Markin and Joseph P. Albanesi. 'Membrane fusion: stalk model revisited'. In: *Biophysical Journal* 82 (2002), pp. 693–712.

[Mia+94] Ling Miao, Udo Seifert, Michael Wortis and Hans-Günther Döbereiner. 'Budding transitions of fluid-bilayer vesicles: the effect of area-difference elasticity'. In: *Phys. Rev. E* 49 (1994), pp. 5389–5407.

[MN14] Fernando C. Marques and André Neves. 'Min-max theory and the Willmore conjecture'. In: *Annals of Mathematics* 179.2

(2014), pp. 683–782. DOI: 10.4007/annals.2014.179.2.6. arXiv: 1202.6036 [math.DG].

[MS20] Andrea Mondino and Christian Scharrer. 'Existence and regularity of spheres minimising the Canham–Helfrich energy'. In: *Archive for Rational Mechanics and Analysis* 236.3 (2020), pp. 1455–1485. DOI: 10.1007/s00205-020-01497-4.

[PR13] Dušan Pokorný and Jan Rataj. 'Normal cycles and curvature measures of sets with d.c. boundary'. In: *Advances in Mathematics* 248 (2013), pp. 963–985. DOI: 10.1016/j.aim.2013.08.022. arXiv: 1209.2305 [math.DG].

[RSS24] Fabian Rupp, Christian Scharrer and Manuel Schlierf. *Gradient flow dynamics for cell membranes in the Canham–Helfrich model*. Version 2. To appear in Arch. Ration. Mech. Anal. 2024. arXiv: 2408.07493 [math.AP].

[SAH25] Leonhard J. Starke, Christoph Allolio and Jochen S. Hub. 'How pore formation in complex biological membranes is governed by lipid composition, mechanics, and lateral sorting'. In: *PNAS Nexus* 4.3, pgaf033 (2025). DOI: 10.1093/pnasnexus/pgaf033.

[Sch12] Johannes Schygulla. 'Willmore minimizers with prescribed isoperimetric ratio'. In: *Archive for Rational Mechanics and Analysis* 203.3 (2012), pp. 901–941. DOI: 10.1007/s00205-011-0465-4. arXiv: 1103.0167 [math.DG].

[SE97] D. P. Siegel and R. M. Epand. 'The mechanism of lamellar-to-inverted hexagonal phase transitions in phosphatidylethanolamine: implications for membrane fusion mechanisms'. In: *Biophysical Journal* 73.6 (1997), pp. 3089–3111. DOI: 10.1016/S0006-3495(97)78336-X.

[SG00] U. S. Schwarz and G. Gompper. 'Stability of inverse bicontinuous cubic phases in lipid-water mixtures'. In: *Physical Review Letters* 85 (2000), pp. 1472–1475.

[She+06] G. C. Shearman, O. Ces, R. H. Templer and J. M. Seddon. 'Inverse lyotropic phases of lipids and membrane curvature'. In: *Journal of Physics: Condensed Matter* 18 (2006), S1105–S1124.

[Sie93] D. P. Siegel. 'Energetics of intermediates in membrane fusion: comparison of stalk and inverted micellar intermediate mechanisms'. In: *Biophysical Journal* 65.5 (1993), pp. 2124–2140. DOI: 10.1016/S0006-3495(93)81256-6.

[SK04] D. P. Siegel and M. M. Kozlov. 'The Gaussian curvature elastic modulus of N-monomethylated dioleoylphosphatidylethanolamine: relevance to membrane fusion and lipid phase behaviour'. In: *Biophysical Journal* 87 (2004), pp. 366–374.

[SW25] Christian Scharrer and Alexander West. 'On the minimization of the Willmore energy under a constraint on total mean curvature and area'. In: *Archive for Rational Mechanics and Analysis* 249.2

(2025). DOI: 10.1007/s00205-025-02087-y. arXiv: 2403.14579 [math.DG].

[Wan+24] Mei-Ting Wang, Gao-Xiao Jiang, Rui Ma and Chen-Xu Wu. *Determination of Gaussian curvature modulus and spontaneous curvature via membrane buckling.* 2024. DOI: 10.1101/2024.12.27.630512.

[Wil65] T. J. Willmore. 'Note on embedded surfaces'. In: *An. Şti. Univ. "Al. I. Cuza" Iaşi* 11B (1965), pp. 493–496.

Email address: sotofranco.eng@gmail.com